Faraday Discussions

ARTICLE

Structure-Activity Relationships for the Solid State Emission of a New Family of "Push-Pull" π-Extended Chromophores

Andrea Nitti,[a] Francesca Villafiorita-Monteleone,[b] Aurora Pacini,[a] Chiara Botta,[b] Tersilla Virgili,[c] Alessandra Forni,[d] Elena Cariati,[e] Massimo Boiocchi,[f] and Dario Pasini[*,a]

We report on the design, synthesis, molecular optical properties, and solid state emissive behaviour of a series of novel compounds, which, similarly to the archetypal AIE luminogen tetraphenylethene, are formed by a central olefin stator and decorated with either three or four rotors; the rotors, being either electron-rich substituted benzenes, or electron-withdrawing functional groups (esters, ketones, cyano groups) confer "push-pull" character to the overall molecular structure. Building on both new and already published contributions, a comprehensive picture of the properties and the potential of these compounds is provided.

Introduction

Strong emission in the aggregated state for organic compounds have long been considered counterintuitive: aggregation-caused quenching (ACQ) takes place in the condensed phases for most π–extended, emitting chromophores. ACQ severely inhibits their applications in real-world devices, such as light-emitting diodes, optical waveguides and lasers.[1] In recent years, Tang and other groups have demonstrated that selected organic dyes can indeed behave in the counterintuitive way: they are non-emissive when in diluted solutions, and become highly emissive in the solid state.[2]

Many molecular systems have been proven to be efficient AIE luminogens; one of the prototypical AIE emissive chromophores, and the first one to have been reported, is hexaphenyl-substituted silole (HPS), published by Tang and coworkers in 2001.[3] Aggregation-induced emission (AIE) is frequently ascribed to restricted internal rotations (RIR):[4] for example, when HPS is in solution, the rotations of its phenyl rings dissipate the excitation energy, whereas the aggregate formation in crystals does not allow the phenyl ring rotations and a radiative decay with the nanosecond lifetime is activated. Apart from the silole systems, a great deal of work has been done with other AIE luminogens, aiming at confirming and exploiting the RIR principle. To date, many other families of compounds have since been proposed, featuring a variety of scaffold functionalitites and different "switching on" mechanisms for emission in the solid state. The field has been recently and comprehensively reviewed.[5]

The most widely used amongst the prototypical AIE chromophore families is tetraphenylethene (TPE), which has been extensively investigated. The central olefin stator of the molecule is surrounded by four peripheral aromatic rotors (the phenyl rings). Its high solid state quantum yield, and its relatively simple synthesis have prompted its inclusion in a wide variety of complex architectures, such as linear[6] and hyperbranched polymers,[7] and metal-organic frameworks.[8] In most, cases, the high solid state efficiency of the molecular scaffold is fully preserved by the introduction of the organic functionalities needed for the its covalent or noncovalent bridging to the macromolecular/supramolecular architectures. In other words, the TPE scaffold is able to withhold AIE activity even if major modifications are inserted within its chemical structure.

D–π–A dyes usually exhibit unique emissive properties due to their intramolecular charge transfer (ICT) transitions, and they are of great potential interest since ground and excited electronic states can be tuned under various conditions.[9] We have serendipitously discovered a new class of AIE luminogens with a "push-pull" structure. They possess similarities to TPE, since the central stator is still a carbon-carbon double bond, which is decorated with three (and not four as in TPE) substituents, two carboxylate esters and a 4-dialkylaminophenyl branch (Figure 1, compounds series **1**).[10] Studying in detail one of the AIE active compounds using ultrafast pump–probe spectroscopy combined with calculations, we have given direct evidence that RIR is the key process for switching on the AIE properties.[11]

[a.] Department of Chemistry and INSTM Research Unit, University of Pavia, Viale Taramelli, 10, 27100 Pavia, Italy. Email: dario.pasini@unipv.it
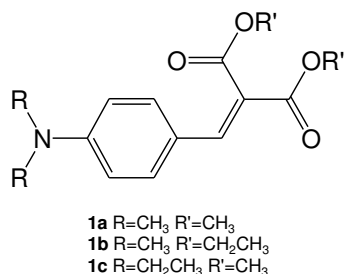[b.] ISMAC -CNR, Via Corti 12, 20133 Milano, Italy
[c.] IFN-CNR, Dipartimento di Fisica, Politecnico di Milano, Piazza Leonardo Da Vinci, 32, 20132 Milano, Italy
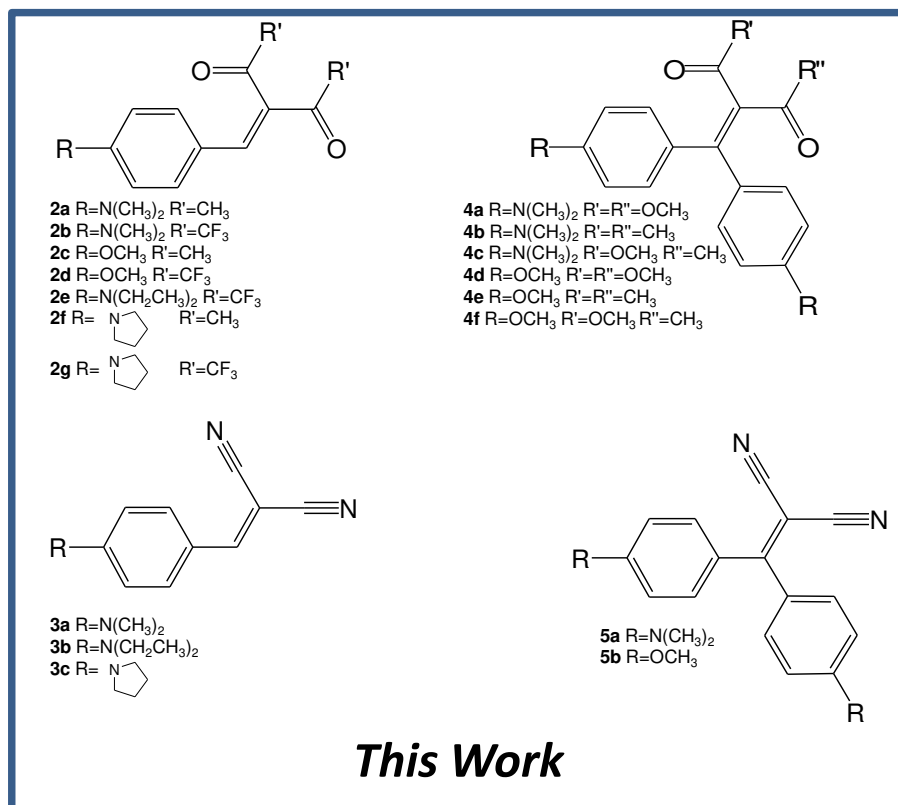[d.] ISTM - CNR, c/o Dipartimento di Chimica, Università degli Studi di Milano, Via Venezian, 21, 20133 Milano, Italy
[e.] Università degli Studi di Milano, Dipartimento di Chimica, via Golgi 19, 20133 Milano, Italy
[f.] Centro Grandi Strumenti, University of Pavia, Via Bassi, 21 - 27100 - Pavia, Italy

Fig. 1. Chemical structure of compound series **1-5**.

More recently, compound **2b** (Figure 1) was effective in unraveling important features of the twisted intramolecular charge transfer mechanism, a peculiar characteristic of such "push-pull" structures.[12]

The potential for such molecular scaffolds for the design of innovative AIE luminogens is huge, since the molecular optical properties (absorption and emission λ_{max}), and consequently the solid state emission, can in principle be tuned by using "push" and "pull" substituents with variable electron-donating and electron-withdrawing characters. In fact, we have recently reported that one of these compounds (**5a** in Figure 1) crystallizes in four different polymorphs all showing different emission colors, and that the emission color can be tuned by heating and grinding in the solid state, highlighting potential applications as stimuli responsive solid-state materials.[13]

In this paper, we report our further achievements into a fine tuning of the previously proposed molecular "push-pull" structures, in order to investigate the potential in terms of AIEs, to match requirements for optoelectronics and sensing applications. We will discuss the optical properties, and the AIE and solid state behavior of a series of compounds in which the original molecular structure has been systematically varied (Figure 1). Together with the mentioned electronic characteristics of the rotor groups around the stator, necessary to give "push-pull" character, given the importance of the RIR mechanism, variations of the steric hindrance of the rotor functional groups around the stator have also been addressed.

Results and discussion

Design and synthesis of the molecular modules

The compounds presented and discussed in this study are shown in Figure 1. For sake of clarity we have divided them into five different classes (compounds **1-5**). Compound series **1** have been already reported, and possess ester derivatives as the "pull" components in a trisubstituted ethylene molecular scaffold; they bear minimal differences amongst them, either in the nature of the alkyl ester substituents, or in the nature of the dialkyl amino substituents. In compounds series **2**, the "pull" ester moieties have been changed with ketones and trifluoromethylketones, both possessing a similar degree of steric hindrance with respect to esters, but with substantially different electron-withdrawing characteristics, as testified by their the σ_p Hammett parameters[14] (0.45 for COOCH$_3$, 0.50 for COCH$_3$, and 0.80 for COCF$_3$). Further, in compound series **2**, the "push" dimethylamino group has been changed in two complementary ways: a) it has been substituted with a methoxy group; b) it has been changed with linear or cyclic dialkylamino groups, addressing differences in the packing properties in the solid state. The importance of the length of the dialkylamino substituent have been already demonstrated in compound series **1**, where a switching off of the AIE properties had been observed by changing dimethylamino with diethylamino "pull" moieties.[10a]

ARTICLE

Compound series **3** has been designed with cyano substitutents, linear functional groups with low steric hindrance, and possessing different electronic characteristics with respect to esters or ketones (σ_p = 0.66). Variable dialkylamino substituents has been also synthesized in this series. The introduction of a further dimethylaminoaryl "pull" moiety into the molecular skeleton, to form tetrasubstituted ethylene, "cruciform-like" derivatives,[15] has been synthetically achieved (series **4** and **5**).

The synthesis of compounds **2-3** has been carried out following adaptations of reported conditions starting from the appropriate aldehyde and the 1,3-dicarbonyl compound or malononitrile. An initial screening of optimal conditions has been performed for the synthesis of compound **2a**, which has been previously reported. Yields using the reported procedure,[16] with piperidinium acetate as the catalyst, were somehow disappointing (17%). Other published methods (CuCl$_2$ a the catalyst)[17] for unsubstituted benzaldehyde were equally not satisfactory (17%), whereas the use of an excess of acetic anhydride (procedure published for the synthesis of the previously known **2d**)[18] gave improved yields (25% for **2a**). The last methodology was then applied to all compounds **2** and **3**, with satisfactory yields, ranging, after purification by column chromatography, from 25% to 76% (Scheme 1, top).
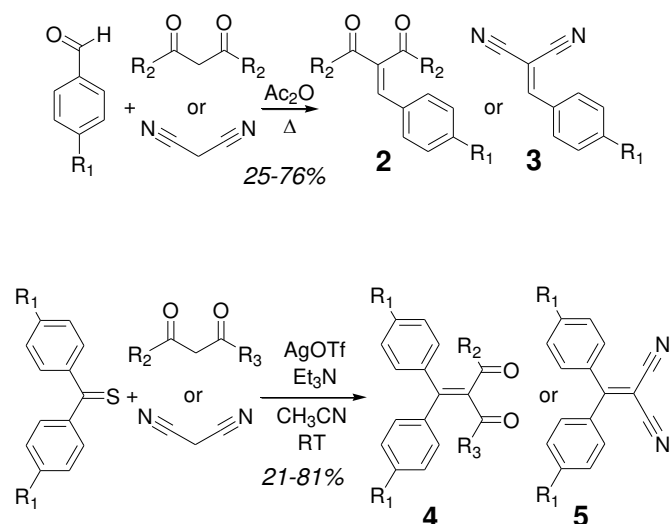
Scheme 1. Synthesis of compound series **2-5**.

Compound series **4** and **5** were synthesized by silver triflate mediated condensation[19] of the appropriate 4,4'-disubstituted thiobenzophenone (either commercially available or *ad hoc* synthesized from the corresponding dibenzophenone with Lawesson's reagent[20]), and the appropriate 1,3-dicarbonyl compound or malononitrile (Scheme 1, bottom). Yields after purification by column chromatography were satisfactory, ranging between 21 and 81%. All new compounds were fully characterized by NMR spectroscopy and mass spectrometric techniques.

The room temperature ^{1}H NMR spectra for all compounds showed the expected simple patterns and the presence of only one set of signals for each group of symmetry-related proton resonances, revealing that all possible dynamic processes are fast on the NMR timescale at this temperature. Comparison between relevant signals of their ^{1}H and ^{13}C NMR spectra are presented in Tables S1-S4 in the Supporting Information section. No evidence of enol structures could be found in the spectra of compounds **2a** and **2c**, and **4b**, **4c**, **4e**, **4f**, bearing hydrogen atoms α to a carbonyl and thus supporting the possibility of enolization: signals related to the CH$_3$ groups integrate correctly with respect to the rest of the proton resonances, and no vinyl signals in the appropriate region (5-6 ppm) could be detected.

The locking of the rotation of the "pull" moieties (for example, ester and ketones in compounds **1a** and **2b**, respectively) and of the aryl moiety around its own axis are both key elements responsible for the molecular ridigification and the activation of the RIR mechanism in solid-state emission.[10a,11,12] Compounds **3a** and **5a** possess linear cyano moieties, for which any lateral steric interaction is not possible, as the "pull" components, and thus can be ideal models for the investigation of the "pirouetting" movements of the aryl moieties. Variable Temperature NMR studies performed on compound **3a** revealed that this molecular rotation becomes slow on the NMR timescale (Figure 2) upon freezing the sample in d_8-THF. At low temperatures the Hb protons, split into two different signals, as a result of the loss of the local symmetry around the aryl main axis, which coalesce at 213 K. A free energy barrier for such dynamic process (9.6 kcal mol^{-1}) could be calculated with the coalescence method.[21]
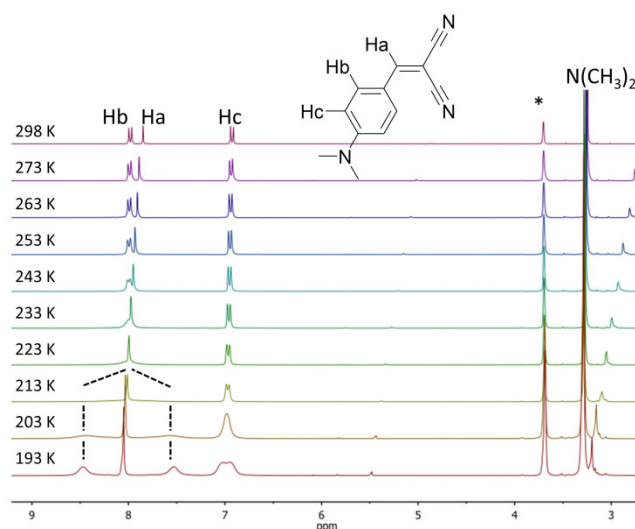

Fig. 2. Variable Temperature ^{1}H NMR spectra (300 MHz, d_8-THF) of compound **3a**. The asterisk denotes residual solvent peak.

For compound **5a** such signal splitting could not be observed down to 193 K (Figure S1), so that a precise value for the energy barrier for the rotation of the aryl rings around their axes, to compare with **3a**, could not be calculated.

Molecular optical properties

Relevant optical properties for the compounds discussed are reported in Table 1 in order to rationalize their optical-structural relationship. The λ_{max}, corresponding to the HOMO-

LUMO energy, for homologous series of compounds bearing tha same electron-donating substituent was found to be modulated by the nature of the electron-withdrawing substituent. In fact, a linear correlation between the with σ_p Hammett's parameters of the "pull" moiety (Figure 3) and the λ_{max} for compounds **1a, 2a, 2b, 3a**, all bearing dimethylamino groups, was found. Such correlation indicates a "through bond" effect of the substituents, and demonstrates an effective conjugation through the π-systems, formally composed of a styrene-like moiety. A similar linear correlation (based on the compounds **4a, 4b** and **5a**) could be verified for cruciform-like compounds (Figure S2).
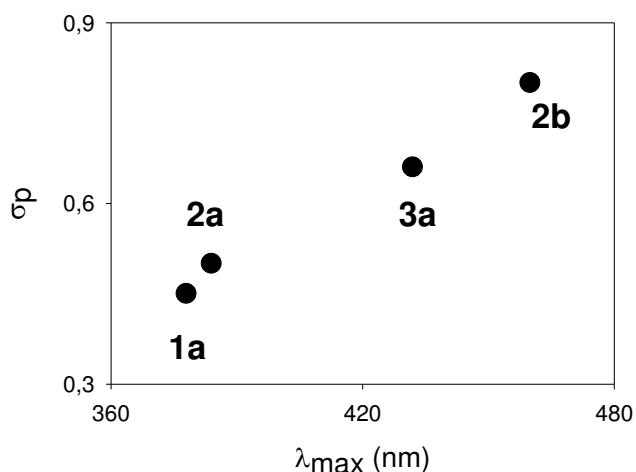

Fig. 3. Correlation between λ_{max} and σ_p Hammett's parameters for dimethylamino-terminated compounds **2** and **3** (fitting coefficient r^2 = 0,99).

Such correlations could also be useful in predicting the properties of analogous compounds utilizing different "push-pull" substituents. The direct comparison, where possible, between monoaryl systems (classes **2** and **3**) and cruciform-like systems (classes **4** and **5**) demonstrate (Table 1) that the introduction of a further aryl branch does not enhance the λ_{max} and the "push-pull" character of the system (compare for example **3a** *vs* **5a**, and **1a** *vs* **4a**).

All the compounds reported in Table 1 show a very low PL QY in solution, that does not depend much on the polarity of the solvent. Compounds **1a**,[10a] **2b**,[12] **2e**, **3a**, **3b** and **5a**[13] show solvatochromic behaviours related to their push-pull molecular structure (see SI) without any relevant variation of the emission intensity. However, for compounds **1a** and **2b**, a strong increase of the PL intensity by increasing the solvent viscosity has been observed[10a,11b] indicating that the rigidity of the environment, rather than its polarity, plays an important role in their emissive process. By freezing the solutions or by adding a non-solvent to the solutions, we have reported an increase of the PL intensity for compounds **1a** and **5b**.[10a,12] In diluted solutions, below the solidification point of the solvent, the molecular motions are blocked by the rigidified solvent. Upon adding a non-solvent at room temperature to the diluted solutions, molecular aggregation into nanoparticles blocks the intramolecular motions. Their AIE properties have been therefore ascribed to the commonly observed RIR effect.

Table 1. Optical properties of compound series **1-5** in solution and as powders.

Compound	λ_{abs} (nm)[a]	λ_{em} (nm), solution[b]	λ_{em} (nm), powder	PLQY (%), solution	PLQY (%), powder	Physical Appearance
1a	378	429[c]	468	<0.1	38	**Solid**
1b	380	440[c]	473	<0.1	38	**Solid**
1c	380	445[c]	522	<0.1	1	**Solid**
2a	382	462	520	0.33	1	**Solid**
2b	461	553	625	<0.1	11	**Solid**
2c	274	n.a	n.a.	n.a	n.a.	**Oil**
2d	360	n.a	n.a.	n.a	n.a.	**Oil**
2e	467	528	630	<0.1	<0.1	**Solid**
2f	390	456	540	1	<0.1	**Solid**
3a	430	488	615	0.9	3	**Solid**
3b	436	491	550,630	1.4	5	**Solid**
3c	436	491	630	0.87	3	**Solid**
4a	360	n.a	n.a.	n.a	n.a.	**Oil**
4b	385	495	500	<0.1	<0.1	**Solid**
4c	384	495	512	0.1-1	1	**Solid**
5a	432	511	530, 535,595	<0.1	11[d]	**Solid**
5b	337	395	480	<0.1	5	**Solid**

[a] In MeCN solutions (1-5 10^{-5} M). [b] Emission maximum, solutions 10^{-6} M. [c] Data taken from ref. 10a, in toluene. [d] max PL QY of the polymorphs.

Faraday Discussions

ARTICLE

As shown in Table 1, some of the compounds display a strong enhancement of the PL QY in the solid state, while others maintain nearly the same low values of the solutions. Compounds **1a** and **1b** display the strongest PL enhancement, compounds **3** and **5** a moderate one while in the case of compounds **4** and **2** (with the exception of **2b**) no relevant variations are observed in the PL intensity from the solution to the solid state. Changes in the lateral alkyl chains in the "push" moieties bring about substantial changes in the AIE properties: on going from dimethylamino to diethylamino aryl substituents the AIE behaviour is either strongly reduced (from **1a** to **1c**) or switched off (from **2b** to **2e**) . In the case of **3a** (dimethylamino, already not AIE) the change to diethylamino (**3b**) confirms the absence of AIE behaviour.

Among the others, compounds **3b** and **5a** display quite interesting features, with solvatochromism in solution, good solid state QY and the presence of different components in the solid state emission, already studied in detail in the case of compound **5a**.[12] The optical absorption, PL excitation profiles (PLE) and emission spectra of **3b** in acetonitrile solution and as powders are reported in Figure 4. For powders, a strong red-shift in the PL and the presence of two peaks (495 and 580 nm) in the PLE spectra are observed. The latter ones are very probably associated to the presence of two different species which can be separated thanks to their different solubilty in pentane. Upon pentane extraction two main contributions are observed in the emission spectrum, a shoulder at 550 nm and the main peak at 630 nm while the insoluble portion of the powders displays a main emission at 635 nm. The relative intensity of the two contributions can be changed upon manual grinding of the powders (see SI).
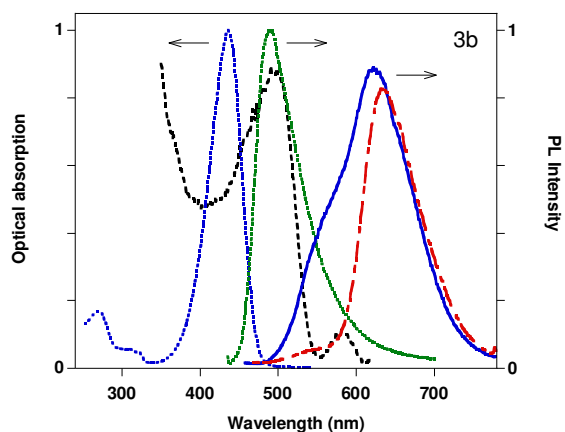

Fig. 4. Optical absorption and PL spectra of compound **3b** in acetonitrile solution (dotted lines). PLE and PL spectra of solid **3b**: pentane soluble component (solid line) and pentane unsoluble component (dashed-dotted line).

Since for RIR materials the emissive properties strictly depend on the type of aggregation (crystalline vs amorphous) and on the crystal rigidity, in the next section we analyse the crystal structures of the compounds in detail.

X-Ray crystal structures

Crystal structures of compounds **1**,[10a] **2b**,[12] and **5a**[13] were previously reported by us together with a thorough discussion, supported by DFT and TDDFT calculations,[11-13] of the structure-optical properties relationships governing their emissive behaviour. It was found that their AIE properties were strictly related to their crystal structure that is able to activate a RIR process. Moreover, by comparing the crystal structures and the solid state optical behaviours of the different compounds, we have ascribed the high PL QY (up to 38%) observed for compounds **1a** and **1b** to the formation of J-dimers.

Unlike the molecular structures of the previously reported compounds, those of compounds **3** (**3a**[22] and **3b**[23] previously reported) are essentially planar. Crystals of **3c** belong to the P-1 space group with 6 molecules in the asymmetric unit (see Figure 5 for crystal packing). A subtle, not previously highlighted, feature shared by these structures, which could have some role in their emissive behaviour, was the slightly greater conjugation degree of the *trans* CN group with the benzene ring with respect to the *cis* one. The angles between the CN bonds and the normal to the plane through the benzene ring were in facts 88.9(1)° (**3a**[22c]) and in the range 85.9(2)-89.5(2)° (**3c**) for the *trans* CN group and 79.5(1)° (**3a**) and in the range 77.6(2)-85.3(2)° for the *cis* one. In the case of **3b**[23b] the two angles were comparable (84.8(1) and 86.7(1)°, respectively).

The crystal structures of **3** share a pseudo layered structure, but **3a** and **3b** do not reveal the presence of significant π-π stacking interactions owing to too long interplanar distances between adjacent benzene rings. Only C–H···N (**3a**) or C–H···N and C–H···π (**3b**) intermolecular interactions stabilize their crystal structures. In the case of **3c**, besides C–H···N and C–H···π interactions, we observe also short CC contacts (3.337 and 3.317 Å) involving however only 4 of the 6 independent molecules. As a result, the presence of weak interactions in crystal phase explains the AIE behaviour of compounds **3**, while their rather low PL QY can be ascribed to the absence of strong aggregates (Figure 5).
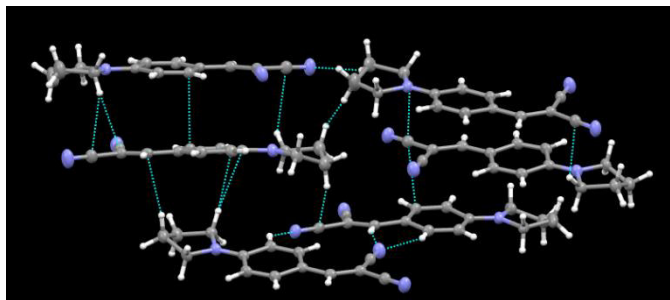
Fig. 5. Partial view of the crystal packing of **3c**, where contacts shorter than the sum of van der Waals radii are included. Ellipsoids are drawn at the 50% probability level.

Crystals of **5b** belong to the C2/c space group with half a molecule in the asymmetric unit (see Figure 6). Unlike **5a**, for which four kinds of crystals were obtained, characterized by different morphologies and absorption and emission colours, only one phase was obtained for **5b**. A distinctive feature of these molecular structures is their twisted conformation due to sterical hindrance both between the CN and the dimethylamino-phenyl substituents and between the phenyl rings. As previously evidenced,[12] three geometrical factors can play in a concerted way to reduce such hindrance, that is, the (N)C–C=C–C(Ph) torsion angle, the reciprocal tilting of the phenyl rings (quantified through the dihedral angle between the least-squares planes through the phenyl carbon atoms) and the central double bond, which in the present structures is significantly elongated with respect to the value of 1.331(9) Å reported for (C_2)–C=C–(C_2) unconjugated bonds,[24] denoting a high conjugation degree. It is to be pointed out that, owing to their cross-conjugated architecture,[25] the phenyl rings, connected with each other by two single bonds, are separately conjugated to each CN group, as well as the CN groups are separately conjugated to each phenyl ring. The conformational differences observed in the four crystals of **5a**, though small, were found to be associated with a different conjugation degree between the molecular moieties connected through the C=C double bond. In particular, the lower the dihedral angle between the phenyl rings, the larger the distortion around the double bond and greater the cross-conjugation. In the case of **5b**, we observe a large dihedral angle between the phenyl rings (71.6(1) vs. 71.8(1)-58.0(1)° found in **5a**), a lower (N)C–C=C–C(Ph) torsion (9.0(1) vs. 11.8(1)-19.9(1)° of **5a**) and a shorter C=C bond length with respect to **5a** (1.366(3) vs. 1.376(3)-1.390(2) Å, respectively). All these features indicate a lower cross-conjugation for **5b** with respect to **5a**.

The twisted conformations of compounds **5** rule out the presence of strong intermolecular π–π stacking interactions, excluding the formation of H- or J-aggregates. On the other hand, as noted for compounds **3**, the weak C–H···N and C–H···π intermolecular interactions found in structures of **5a** and **5b** are enough to fix the molecular conformations in the crystal structures activating the RIR mechanism. In both **3** and **5** series of compounds, the absence of strong intermolecular interactions and the conformational freedom associated with the presence of several single bonds explain the formation of different polymorphs, as demonstrated by X-ray

investigation for **5a** and suggested from spectroscopic evidence for **3b**.
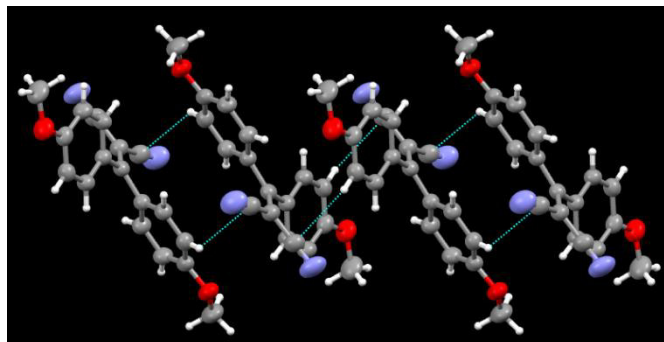

Fig. 6. Partial view of the crystal packing of **5b**, where contacts shorter than the sum of van der Waals radii are included. Ellipsoids are drawn at the 50% probability level

Pump-probe experiments

A deep understanding of the role of the intramolecular torsional mobility in AIE molecules is of crucial importance in order to design new organic compounds with improved optoelectronic properties. We reported on the spectral evolution of the stimulated emission of compounds **1** dissolved in solution showing that the torsional relaxation toward the equilibrium geometry of the excited state takes place on time scales that depend on the solvent viscosity.[11] Pump-probe ultrafast dynamic has been also employed to study the time evolution of the excited states of compound **2b** whose long-living optical gain was detected only when the twisted intramolecular charge transfer mechanism is inhibited by increasing the solvent viscosity.[12]

Here we report ultrafast pump-probe measurements on two solutions of compound **5a** displaying different viscosity, namely Polyethylene glycol (PEG) and acetonitrile (ACN) In this way it is possible to temporally resolve the spectral evolution of the excited states created after the pump excitation of the molecule dispersed in viscous and non-viscous solvents. In this experiment, the transmission of a white light pulse (probe) is detected at different time delays with respect to the pump excitation (400 nm). The differential transmission spectra of the probe pulse ΔT/T (where ΔT = T_{on}-T, being T_{on} the transmission of the probe light with the pump excitation and T the transmission of the probe light without the pump excitation) taken at different probe delays is then obtained. Positive ΔT/T signal (transmission increasing after pump excitation) is an indication of bleaching of the ground state when the signal spectrally overlaps the absorption spectrum or of Stimulated Emission (SE) from the excited state when the signal overlaps the PL spectrum of the molecule. The time-resolved spectra recorded (Fig. 7) in both solvents show a positive broad band that can be associated to Stimulated Emission (SE peak at around 530 nm). In the ACN solution after around 1 ps the formation of a negative Photoinduced Absorption (PA) band centered at 520 nm is observed, displaying a fast decay in few ps time scale (red line, inset

Figure 7b). On the contrary, in PEG solution there is no formation of PA band in time (black line, Inset Figure 7a).
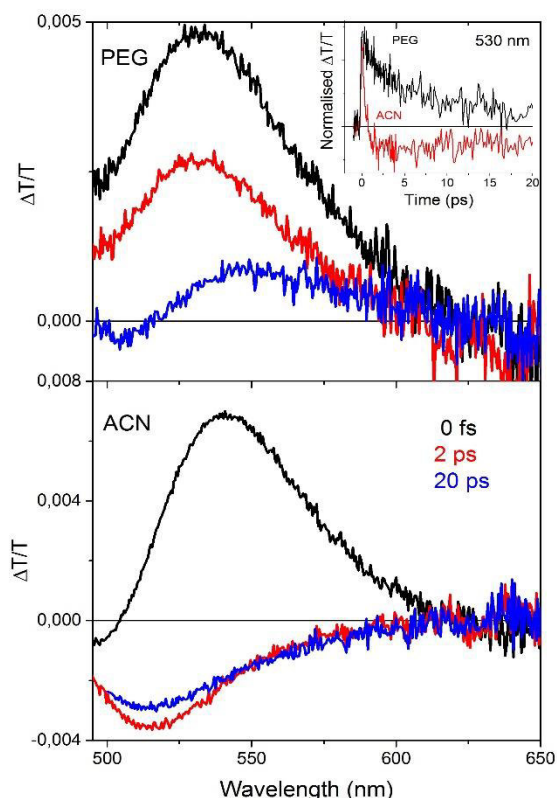

Fig. 7. Differential transmission spectra at 0 fs (black line),2 ps (red line) and at 20 ps (blue line) probe delays for the PEG (top panel) and ACN (bottom panel) solutions.

Conclusions

We have reported and compared the design, synthesis, molecular optical properties, and solid state emissive behaviour of several series of novel compounds with "push-pull" character. The compounds bear three or four substituents around a central olefin stator. While all the structures are non-emissive in solution, a handful of them possess solid-state emissions with quantum yields over 10%. With the exception of compound **5a**, all the AIE compounds are characterized by having three substituents around the stator. As a general trend, the use of 4-methoxyaryl substituents as the "push" component does not bring any useful solid-state emissive behavior.

Our classes of compounds is unique in terms of tunability of emission response, but the translation of molecular design into efficient solid state emission is far from being straightforward. The nice correlations with Hammett's parameters demonstrate the possibility to predict and rationally tune energy gaps for these structures. However, good solid state emissions are activated or disactivated by subtle changes in the molecular structures, sometimes in unpredictable ways. As such, the potential incorporation of the most promising of the structures presented here into complex covalent scaffolds

(polymers, covalent organic frameworks) for functional applications cannot at present considered as immediate as it occurs with other AIE scaffolds.

Experimental

General Experimental for synthesis. All available compounds were purchased from commercial sources and used as received. Compounds **2b**[12] and **5a**[13] were previously reported by us. THF (Na, benzophenone), Et_2O (Na, benzophenone) and CH_2Cl_2 (CaH_2) were dried and distilled before use. ^{1}H and ^{13}C NMR spectra were recorded from solutions in $CDCl_3$ on Bruker 200 or AMX300 with the solvent residual proton signal as a standard. Analytical thin layer chromatography was performed on silica gel, chromophore loaded, commercially available plates. Flash chromatography was carried out using silica gel (pore size 60 Å, 230-400 mesh). ^{1}H and ^{13}C NMR spectra were recorded from solutions in $CDCl_3$ on 200 300 MHz or 500 MHz spectrometer with the solvent residual proton signal or tetramethylsilane as a standard. Mass spectra were recorded using an electrospray ionization instrument (ESI). Melting points are uncorrected.

General procedure for the synthesis of compounds 2 and 3. A solution of the appropriate aldehyde (1 equiv) and ketone or malononitrile (1 equiv) in Ac_2O (5-10 mL) was heated under reflux (140 °C) for 18 h. After cooling to room temperature, the reaction mixture was poured into water/ice, and the aqueous suspension extracted with CH_2Cl_2. The organic phase was washed with a saturated solution of $NaHCO_3$ and then dried (Na_2SO_4). The product was isolated after purification by column chromatography.

Compound 2a. From 4-dimethylaminobenzaldehyde (1.5 g, 10 mmol) and 2,4-pentanedione (1 mL, 10 mmol). Purified by column chromatography (SiO_2; hexanes : AcOEt = 7: 3) and obtained as a yellow-orange solid (572 mg, 25%). R_f = 0.3 (hexanes : AcOEt = 7: 3). ^{1}H-NMR ($CDCl_3$, 200 MHz, 25 °C) δ = 7.40 (s, 1H; Vinyl C*H*), 7.31 (d, 2H; J = 9 Hz, Ar*H*), 6.65 (d, 2H; J = 9 Hz, Ar*H*), 3.05 (s, 6H; -N(C*H$_3$*)$_2$), 2.39 (s, 3H; -COC*H$_3$*), 2.37 (s, 3H; -COC*H$_3$*). ^{13}C NMR ($CDCl_3$, 75 MHz, 25°C) δ = 207.0 (C_q), 196.3 (C_q), 151.8 (C_q), 140.9 (vinyl C_H), 137.8 (C_q), 132.2 (Ar CH), 120.1 (C_q), 111.8 (Ar CH), 40.0 (N(CH$_3$)$_2$), 31.6 (CH$_3$), 26.1 (CH$_3$). MS-ESI *m/z* (%) = 232 [*M* + H]$^+$ (100), 485 [2*M* + Na]$^+$ (70) The crystal structure of this compound has been previously reported.[26] The ^{1}H and ^{13}C NMR spectra matched those previously reported.[27]

Compound 2c. From 4-methoxybenzaldehyde (610 µL, 5 mmol) and 2,4-pentanedione (516 µL, 5 mmol). Purified by column chromatography (SiO_2; hexanes : AcOEt = 9: 1) and obtained as a yellow oil (255 mg, 25%). R_f = 0.14 (hexanes : AcOEt = 9: 1). ^{1}H-NMR ($CDCl_3$,200 MHz, 25°C) δ = 7.63 (s, 1H; Vinyl C*H*), 7.47 (d, 2H; J = 9 Hz, Ar*H*), 6.93 (d, 2H; J = 9 Hz; Ar*H*), 3.83 (s, 3H; -OC*H$_3$*), 2.12 (m, 6H; 2C*H$_3$*). The ^{1}H NMR spectrum matched those previously reported.[28]

Compound 2d. From 4-methoxybenzaldehyde (1.2 mL, 10 mmol) and hexafluoroacetylacetone (1.4 mL, 10 mmol). Purified by column chromatography (SiO_2; hexanes : CH_2Cl_2 = 7: 3) and obtained as a

yellow oil (925 mg, 28%). R_f = 0.3 (hexanes : CH_2Cl_2 = 7: 3). ^{1}H-NMR (CDCl$_3$,200 MHz, 25°C) δ = 7.99 (s, 1H; Vinyl C*H*), 7.42 (d, 2H; *J* = 9 Hz; Ar*H*), 6.97 (d, 2H; *J* = 9 Hz; Ar*H*), 3.87 (s, 3H; -OC*H*$_3$). This compound was previously reported, but no NMR information was given.[18]

Compound 2e. From 4-diethylaminobenzaldehyde (177.3 mg, 1 mmol) and hexafluoroacetylacetone (142 µL, 1 mmol). Purified by column chromatography (SiO$_2$; hexanes : CH_2Cl_2 = 1: 1) and obtained as a pink waxy solid (185 mg, 50%). R_f = 0.5 (hexanes : CH_2Cl_2 = 1: 1). M.p. = 60-62°C. ^{1}H-NMR (CDCl$_3$,200 MHz, 25°C) δ = 7.83 (s, 1H; Vinyl C*H*), 7.34 (d, 2H; *J* = 9 Hz; Ar*H*), 6.65 (d, 2H; *J* = 9 Hz; Ar*H*), 3.48 (q, 4H; *J* = 7 Hz; 2C*H*$_2$), 1.25 (t, 6H; *J* = 7 Hz; 2C*H*$_3$).

Compound 2f. From 4-pyrrolidinobenzaldehyde (876 mg, 5 mmol) and 2,4-pentanedione (501 mg, 5 mmol). Purified by column chromatography (SiO$_2$; hexanes : AcOEt = 8: 2) and obtained as a orange-brown solid (421 mg, 37%). R_f = 0.3 (hexanes : AcOEt = 8: 2). ^{1}H-NMR (CDCl$_3$,200 MHz, 25°C) δ = 7.40 (s, 1H; Vinyl C*H*), 7.30 (d, 2H; *J* = 9 Hz; Ar*H*), 6.52 (d, 2H; *J* = 9 Hz; Ar*H*), 3.36 (m, 4H; 2C*H*$_2$), 2.38 (s, 3H; C*H*$_3$), 2.37 (s, 3H; C*H*$_3$), 2.04 (m, 4H; 2C*H*$_2$). ^{13}C NMR (CDCl$_3$, 75 MHz, 25°C) δ = 207.2 (C$_q$; -CO), 196.1 (C$_q$; -CO), 149.4 (C$_q$), 141.3(CH), 137.1 (C$_q$), 132.4 (CH), 119.3 (C$_q$), 111.7 (CH), 47.4 (CH$_2$), 31.6 (CH$_3$), 26.1 (CH$_3$), 25.3 (CH$_2$).

Compound 2g. From 4-pyrrolidinobenzaldehyde (876 mg, 5 mmol) and hexafluoroacetylacetone (700 µL, 5 mmol). Purified by column chromatography (SiO$_2$; hexanes : CH_2Cl_2 = 1: 1) and obtained as a dark red solid (512 mg, 28%). R_f = 0.4 (hexanes : CH_2Cl_2 = 1: 1). M.p. = 89-91°C. ^{1}H-NMR (CDCl$_3$, 200 MHz, 25°C) δ = 7.85 (s, 1H; Vinyl C*H*), 7.35 (d, 2H; *J* = 9 Hz; Ar*H*), 6.45 (d, 2H; *J* = 9 Hz; Ar*H*) ,3.45 (t, 4H; 2C*H*$_2$), 2.08 (m, 4H; 2C*H*$_2$). ^{13}C NMR (CDCl$_3$, 75 MHz, 25°C) δ = 187.6 (q, C$_q$; *J* = 35 Hz), 177.5 (q, C$_q$; *J* = 35 Hz), 152.1 (C$_q$), 151.8 (CH), 135.2 (CH), 119.2 (C$_q$), 118.1 (C$_q$), 117.1 (q, C$_q$; *J* = 300 Hz), 115.3 (q, C$_q$; *J* = 300 Hz), 112.4 (CH), 47.8 (CH$_2$), 25.2 (CH$_2$).

Compound 3a. From 4-dimethylaminobenzaldehyde (746 mg, 5 mmol) and malononitrile (330 mg, 5 mmol). Purified by column chromatography (SiO$_2$; hexanes : CH_2Cl_2 = 2: 8) and obtained as an orange solid (388 mg, 40%). R_f = 0.7 (hexanes : CH_2Cl_2 = 2: 8). ^{1}H-NMR (CDCl$_3$,200 MHz, 25°C) δ = 7.83 (d, 2H; *J* = 9 Hz; Ar*H*), 7.48 (s, 1H; Vinyl C*H*), 6.68 (d, 2H; *J* = 9 Hz; Ar*H*), 3.15 (s, 6H; -N(C*H*$_3$)$_2$). ^{13}C NMR (CDCl$_3$, 75 MHz, 25°C) δ = 157.9 (CH), 154.1 (C$_q$), 133.7 (CH), 119.2(C$_q$), 115.9 (C$_q$; -CN), 114.8 (C$_q$; -CN), 111.5 (CH), 71.9 (C$_q$), 40.0 (CH$_3$). The ^{1}H NMR spectrum matched the one previously reported.[29]

Compound 3b. From 4-diethylaminobenzaldehyde (886 mg, 5 mmol) and malononitrile (330 mg, 5 mmol). Purified by column chromatography (SiO$_2$; hexanes : CH_2Cl_2 = 2: 8) and obtained as a dark pink solid (851 mg, 76%). R_f = 0.4 (hexanes : CH_2Cl_2 = 2: 8). ^{1}H-NMR (CDCl$_3$,200 MHz, 25°C) δ = 7.81 (d, 2H; *J* = 9 Hz; Ar*H*), 7.44 (s, 1H; Vinyl C*H*), 6.68 (d, 2H; *J* = 9 Hz; Ar*H*), 3.48 (q, 4H; *J* = 7 Hz; 2C*H*$_2$), 1.25 (t, 6H; *J* = 7 Hz; 2C*H*$_3$). ^{13}C NMR (CDCl$_3$, 75 MHz, 25°C) δ = 157.7 (CH), 152.3 (C$_q$), 134.0 (CH), 118.8(C$_q$), 116.1 (C$_q$; -CN), 114.9 (C$_q$; -CN), 111.2 (CH), 71.0 (C$_q$), 44.8 (CH$_2$), 12.4 (CH$_3$). The ^{1}H and ^{13}C NMR spectra matched those previously reported.[30] The crystal structure of this compound has been previously reported.[23b]

Compound 3c. From 4-pyrrolidinobenzaldehyde (876 mg, 5 mmol) and malononitrile (330 mg, 5 mmol). Purified by column chromatography (SiO$_2$; hexanes : CH_2Cl_2 = 2: 8) and obtained as a brown-orange solid (316 mg, 29%). R_f = 0.55 (hexanes : CH_2Cl_2 = 2: 8). ^{1}H-NMR (CDCl$_3$,200 MHz, 25°C) δ = 7.80 (d, 2H; *J* = 9 Hz; Ar*H*), 7.44 (s, 1H; Vinyl C*H*), 6.57 (d, 2H; *J* = 9 Hz; Ar*H*), 3.45 (m, 4H; 2C*H*$_2$), 2.09 (m, 4H; 2C*H*$_2$). ^{13}C NMR (CDCl$_3$, 75 MHz, 25°C) δ = 157.9 (CH), 151.8 (C$_q$), 133.9 (CH), 119.0(C$_q$), 116.1 (C$_q$), 115.1 (C$_q$), 111.9 (CH), 70.9 (C$_q$), 47.8 (CH$_2$), 25.2 (CH$_2$). This compound was previously reported.[31]

General procedure for the synthesis of compounds 4 and 5. *Preliminary step for compounds 4d-f and 5b.* A solution of 4,4'-dimethoxybenzofenone (1 equiv) and Lawesson's reagent (1.5 equiv) in dry toluene (30 mL) was heated to reflux (110 °C) with a Dean-Stark apparatus for 18 h. The intermediate thioketone was purified by column chromatography, then used without further characterization. *Second step for all compounds 4 and 5.* A solution of the isolated or commercially-available thioketone (1 equiv), the appropriate 1,3-dicarbonyl compound or malononitrile (1.2 equiv), Et$_3$N (3.6 equiv) and AgOCOCF$_3$ (2.5 equiv) in dry CH$_3$CN (6 mL) was stirred in the dark at room temperature for 18 h. The solvent and the base were removed *in vacuo*, the residue partitioned between brine and AcOEt. The organic phase was then dried (Na$_2$SO$_4$), and the product was isolated after purification by column chromatography.

Compound 4a. From 4,4'-bis(dimethylamino)thiobenzofenone (284 mg, 1 mmol), malonic acid methyl ester (137 µL, 1.2 mmol), Et$_3$N (500 µL, 3.6 mmol) and AgOCOCF$_3$ (642 mg, 2.5 mmol) in dry CH$_3$CN (6 mL). Purified by column chromatography (SiO$_2$; hexanes : AcOEt = 8: 2) and obtained as a brown oil (89 mg, 23%). R_f = 0.1 (hexanes : AcOEt = 8: 2). ^{1}H-NMR (CDCl$_3$, 200 MHz, 25°C) δ = 7.12 (d, 4H; *J* = 9 Hz; Ar*H*), 6.54 (d, 4H; *J* = 9 Hz; Ar*H*), 3.76 (s, 6H; -OC*H*$_3$), 2.85 (s, 12H; -N(C*H*$_3$)$_2$). ^{13}C NMR (CDCl$_3$, 75 MHz, 25°C) δ = 168.0 (C$_q$; CO), 158.9 (C$_q$), 151.0 (C$_q$), 131.5 (C$_q$), 127.9 (CH), 118.8 (C$_q$), 111.6 (CH), 51.8 (OCH$_3$), 40.1 (N(CH$_3$)$_2$).

Compound 4b. From 4,4'-bis(dimethylamino)thiobenzofenone (284 mg, 1 mmol), 2,4-pentanedione (123 µL, 1.2 mmol), Et$_3$N (500 µL, 3.6 mmol) and AgOCOCF$_3$ (642 mg, 2.5 mmol) in dry CH$_3$CN (6 mL). Purified by column chromatography (SiO$_2$; CH$_2$Cl$_2$: AcOEt = 9: 1) and obtained as a green emerald solid (109 mg, 31%). R_f = 0.4 (CH$_2$Cl$_2$: AcOEt = 9: 1). ^{1}H-NMR (CDCl$_3$, 200 MHz, 25°C) δ = 7.07 (d, 4H; *J* = 9 Hz; Ar*H*), 6.65 (d, 4H; *J* = 9 Hz; Ar*H*), 3.03 (s, 12H; -N(C*H*$_3$)$_2$), 1.92 (s, 6H; 2COC*H*$_3$). ^{13}C NMR (CDCl$_3$, 75 MHz, 25°C) δ = 204.5 (C$_q$; CO), 154.7 (C$_q$), 151.6 (C$_q$), 132.5 (C$_q$), 127.4 (CH), 126.3 (C$_q$), 111.4 (CH), 40.1 (N(CH$_3$)$_2$), 31.1 (CH$_3$). MS-ESI *m/z* (%) = 351 [*M* + H]$^+$ (100), 723 [2*M* + Na]$^+$ (40).

Compound 4c. From 4,4'-bis(dimethylamino)thiobenzofenone (284 mg, 1 mmol), acetoacetic acid methyl ester (139 mg, 1.2 mmol), Et$_3$N (500 µL, 3.6 mmol) and AgOCOCF$_3$ (642 mg, 2.5 mmol) in dry CH$_3$CN (6 mL). Purified by column chromatography (SiO$_2$; hexanes : AcOEt = 8: 2) and obtained as a yellow solid (190 mg, 52%). R_f = 0.2 (hexanes : AcOEt = 8: 2). ^{1}H-NMR (CDCl$_3$, 200 MHz, 25°C) δ = 7.08 (m, 4H; Ar*H*), 6.63 (m, 4H; Ar*H*), 3.62 (s, 3H; -OC*H*$_3$), 3.01 (m, 12H; 2N(C*H*$_3$)$_2$), 1.88 (s, 3H; C*H*$_3$). ^{13}C NMR (CDCl$_3$, 75 MHz, 25°C) δ =

201.6 (C_q; CO), 169.5 (C_q; $COCH_3$), 156.9 (C_q), 151.7 (C_q), 132.6 (C_q), 131.6 (CH), 127.1 (C_q), 111.1 (CH), 51.7 (OCH_3), 40.0 ($2N(CH_3)_2$), 30.2 (CH_3). MS-ESI m/z = 367 $[M + H]^+$ (100), 755 $[2M + Na]^+$ (70).

Compound 4d. From 4,4'-dimethoxybenzofenone (100 mg, 0.4 mmol) and Lawesson's reagent (243 mg, 0.6 mmol); then 4,4'-dimethoxythiobenzofenone (1 equiv), malonic acid methyl ester (1.2 equiv), Et_3N (3.6 equiv) and $AgOCOCF_3$ (2.5 equiv) in dry CH_3CN (6 mL). Purified by column chromatography (SiO_2; hexanes : AcOEt = 8: 2) and obtained as a white solid (26 mg, 21%). R_f = 0.2 (hexanes : AcOEt = 8: 2). ^{1}H-NMR ($CDCl_3$, 200 MHz, 25°C) δ = 7.12 (d, 2H; J = 9 Hz; ArH), 6.88 (d, 2H; J = 9 Hz; ArH), 3.84 (s, 6H; -$2OCH_3$), 1.93 (s, 6H; $2CH_3$). ^{13}C NMR ($CDCl_3$, 75 MHz, 25°C) δ = 204.0 (C_q; CO), 161.1 (C_q), 150.3 (C_q), 141.3 (C_q), 131.9 (CH), 113.96(CH), 55.3 (OCH_3), 31.1 (CH_3). The compound has been previously reported.[32]

Compound 4e. From 4,4'-dimethoxybenzofenone (100 mg, 0.4 mmol) and Lawesson's reagent (243 mg, 0.6 mmol); then 4,4'-dimethoxythiobenzofenone (1 equiv), 2,4-pentanedione (1.2 equiv), Et_3N (3.6 equiv) and $AgOCOCF_3$ (2.5 equiv) in dry CH_3CN (6 mL) Purified by column chromatography (SiO_2; hexanes : AcOEt = 8: 2) and obtained as a white solid (26 mg, 21%). R_f = 0.2 (hexanes : AcOEt = 8: 2). ^{1}H-NMR ($CDCl_3$, 200 MHz, 25°C) δ = 7.12 (d, 2H; J = 9 Hz; ArH), 6.88 (d, 2H; J = 9 Hz; ArH), 3.84 (s, 6H; -$2OCH_3$), 1.93 (s, 6H; $2CH_3$). ^{13}C NMR ($CDCl_3$, 75 MHz, 25°C) δ = 204.0 (C_q; CO), 161.1 (C_q), 150.3 (C_q), 141.3 (C_q), 131.9 (CH), 113.9 (CH), 55.3 (OCH_3), 31.1 (CH_3).

Compound 4f. From 4,4'-dimethoxybenzofenone (200 mg, 0.8 mmol) and Lawesson's reagent (501 mg, 1.2 mmol); then 4,4'-dimethoxythiobenzofenone (1 equiv), acetoacetic acid methyl ester (1.2 equiv), Et_3N (3.6 equiv) and $AgOCOCF_3$ (2.5 equiv) in dry CH_3CN (6 mL). Purified by column chromatography (SiO_2; hexanes : AcOEt = 8: 2) and obtained as a white solid (60 mg, 34%). R_f = 0.5 (hexanes : AcOEt = 8: 2). ^{1}H-NMR ($CDCl_3$, 200 MHz, 25°C) δ = 7.12 (m, 4H; ArH), 6.86 (m, 4H; ArH), 3.88 (m, 6H; -ArOCH_3), 3.61(s, 3H; COOCH_3), 1.93 (s, 3H; CH_3). ^{13}C NMR ($CDCl_3$, 75 MHz, 25°C) δ = 201.3 (C_q;CO), 168.2 (C_q; $COOCH_3$), 160.7 (C_q), 153.6 (C_q), 132.4 (C_q), 131.9(CH), 131.8 (C_q), 113.9 (CH), 55.3 (OCH_3), 51.9 (OCH_3), 30.3 (CH_3). MS-ESI m/z = 340 $[M]^+$.

Compound 5b. From 4,4'-dimethoxybenzofenone (200 mg, 0.8 mmol) and Lawesson's reagent (501 mg, 1.2 mmol); then 4,4'-dimethoxythiobenzofenone (1 equiv), malononitrile (1.2 equiv), Et_3N (3.6 equiv) and $AgOCOCF_3$ (2.5 equiv) in dry CH_3CN (6 mL). Purified by column chromatography (SiO_2; hexanes : AcOEt = 8: 2) and obtained as a white solid (77 mg, 47%). R_f = 0.2 (hexanes : AcOEt = 8: 2). ^{1}H-NMR ($CDCl_3$, 200 MHz, 25°C) δ = 7.43 (d, 2H; J = 9 Hz; ArH), 6.98 (d, 2H; J = 9 Hz; ArH), 3.89 (s, 6H; -$2OCH_3$). ^{13}C NMR ($CDCl_3$, 75 MHz, 25°C) δ = 173.8 (C_q), 163.3 (C_q), 132.9 (CH), 128.3 (C_q), 114.9(CN), 114.1(CH), 77.4 (C_q), 55.5 (OCH_3). The compound has been previously reported.[33]

Spectroscopical measurements

UV-Vis absorption spectra were obtained with a Perkin Elmer Lambda 900 spectrometer and PL spectra with a SPEX 270 M monochromator equipped with a N2 cooled charge-coupled device exciting with a monochromated 450 W Xe lamp. Spectra were corrected for the instrument response. Photoluminescence quantum yields (PL QYs) of solutions were obtained by using quinine sulfate or coumarine 153 as standards. PL QYs of solid state samples were obtained by using a home-made integrating sphere, as previously reported.[34]

X-ray Crystal Structures

Single crystals of **3c** suitable for X-ray analysis were obtained by CH_2Cl_2/pentane. Diffraction data were collected on a Bruker Smart Apex II CCD area detector using graphite monochromated Mo-Ka radiation. Data reduction was made using SAINT programs; absorption corrections based on multiscan were obtained using SADABS.[35] The structures were solved using SHELXS-97 and refined on F^2 by full-matrix least-squares using SHELXL-14.[36] All the non-hydrogen atoms were refined anisotropically, hydrogen atoms were included as 'riding' and not refined. Crystal data and results of the refinement: orange prism 0.35x0.27x0.25 mm, C14H13N3, M_r = 223.27; triclinic, P-1; a = 10.8613(6) Å, b = 13.0319(7) Å, c = 26.5818(15) Å, α = 89.750(1)°, β = 82.163(1)°, γ = 72.238(1)°, V = 3546.9(3) Å^3; Z = 12; T = 120(2) K; μ(Mo) = 0.077 mm^{-1}. 58049 measured reflections, 15850 independent reflections, 11640 reflections with I > 2σ(I), 1.55 < 2θ < 54.54°, R_{int} = 0.0386. Refinement on 15850 reflections, 928 parameters. Final R = 0.0642, wR = 0.1649 for data with $F^2 > 2\sigma(F^2)$, S = 1.071, $(\Delta/\sigma)_{max}$ = 0.001, $\Delta\rho_{max}$ = 0.668, $\Delta\rho_{min}$ = -0.462 e Å^{-3}.

Single crystals of **5b** suitable for X-ray analysis were obtained by slow evaporation from a $CHCl_3$ solution. Diffraction data were collected on a conventional Enraf-Nonius CAD4 four circle diffractometer, working at ambient temperature with graphite monochromated Mo-Kα Mo Kα X-radiation (λ = 0.7107 Å). Data reduction was performed with the WinGX package.[37] Absorption effects were evaluated with the ψ-scan method[38] and absorption correction was applied to the data. The crystal structure was solved by direct methods (SIR 97)[39] and refined by full-matrix least-square procedures on F^2 using all reflections (SHELXL-14).[36] Anisotropic displacement parameters were refined for all non-hydrogen atoms; hydrogens were placed at calculated positions with the appropriate AFIX instructions and refined using a riding model. Crystal data and results of the refinement: prism 0.75x0.55x0.2 mm, $C_{18}H_{14}N_2O_2$, M_r = 290.31; monoclinic, $C2/c$; a = 17.518(4) Å, b = 8.666(2) Å, c = 10.772(3) Å, β = 110.164(5)°, V = 1535.1(6) Å^3; Z = 4; T = 293(2) K; μ(Mo) = 0.083 mm^{-1}. 2340 measured reflections, 2234 independent reflections, 1378 reflections with $I > 2\sigma(I)$, 4.96 < 2θ < 59.96°, R_{int} = 0.0182. Refinement on 2234 reflections, 129 parameters. Final R = 0.0491, wR = 0.1127 for data with $F^2 > 2\sigma(F^2)$, S = 1.007, $(\Delta/\sigma)_{max}$ = 0.000, $\Delta\rho_{max}$ = 0.170, $\Delta\rho_{min}$ = -0.175 e Å^{-3}.

CCDC 1487807-1487808 contain the supplementary crystallographic data for this paper. These data can be

obtained free of charge from The Cambridge Crystallographic Data Centre via www.ccdc.cam.ac.uk/data_request/cif.

Pump-Probe Experiments

Time-resolved measurements were performed using a home-built femtosecond pump–probe setup. A Ti:sapphire regenerative amplifier (Libra, Coherent) was used as a laser source, delivering 100 fs pulses at a central wavelength of 800 nm with 4 mJ pulse energy at a repetition rate of 1 kHz. For the excitation pulses, we used the second harmonic of the fundamental beam at 400 nm. In order to minimize bimolecular effects, the excitation density was kept at $\approx$ 6mJ/cm2. White light generated with a 2 mm-thick sapphire plate was used as a probe in the visible from 490 to 700 nm. For a spectrally resolved detection of the probe light, a spectrograph and CCD array were used. The chirp in the white light pulse was carefully taken into account during the analysis and evaluation of the obtained two-dimensional (wavelength and time) $\Delta T (\lambda, t)/T$ maps before extraction of the spectral and temporal data with a homemade software. Overall, a temporal resolution of at least 150 fs was achieved for all excitation wavelengths.

Acknowledgements

Notes and references

1 (a) L. Yao, S. Zhang, R. Wang, W. Li, F. Shen, B. Yang and Y. Ma, *Angew. Chem.*, 2014, **126**, 2151; (b) X. Wang, Y. Zhou, T. Lei, N. Hu, E. Q. Chen and J. Pei, *Chem. Mater.* 2010, **22**, 3735; (c) W. Z. Yuan, P. Lu, S. Chen, J. W. Y. Lam, Z. Wang, Y. Liu, H. S. Kwok, Y. Ma and B. Z. Tang, *Adv. Mater.*, 2010, **22**, 2159; (d) H. Uoyama, K. Goushi, K. Shizu, H. Nomura and C. Adachi, *Nature*, 2012, **492**, 234. (e) Q. Liao, H. B. Fu and J. N. Yao, *Adv. Mater.*, 2009, **21**, 4153; (f) J. Y. Zheng, Y. L. Yan, X. P. Wang, Y. S. Zhao, J. X. Huang and J. N. Yao, *J. Am. Chem. Soc.*, 2012, **134**, 2880; (g) X. F. Duan, Y. Huang, R. Agarwal and C. M. Lieber, *Nature*, 2003, **421**, 241.

2 (a) Y. N. Hong, J. W. Y. Lam and B. Z. Tang, *Chem. Soc. Rev.*, 2011, **40**, 5361; (b) Z. Y. Zhang, B. Xu, J. H. Su, L. P. Shen, Y. S. Xie and H. Tian, *Angew. Chem. Int. Ed.*, 2011, **50**, 11654; (c) B. Wang, Y. C. Wang, J. L. Hua, Y. H. Jiang, J. H. Huang, S. X. Qian and H. Tian, *Chem. Eur. J.*, 2011, **17**, 2647; (d) J. Mei, Y. Hong, J. W. Y. Lam, A. Qin, Y. Tang and B. Z. Tang, *Adv. Mater.*, 2014, **26**, 5429.

3 J. D. Luo, Z. L. Xie, J. W. Y. Lam, L. Cheng, H. Y. Chen, C. F. Qiu, H. S. Kwok, X. W. Zhan, Y. Q. Liu, D. B. Zhu and B. Z. Tang, *Chem. Commun.*, 2001, 1740.

4 a) X. Y. Qi, H. Li, J. W. Y. Lam, X. T. Yuan, J. Wei, B. Z. Tang and H. Zhang, *Adv. Mater.*, 2012, **24**, 4191; (b) Z. Li, Y. Q. Dong, J. W. Y. Lam, J. X. Sun, A. J. Qin, M. Häußler, Y. P. Dong, H. H. Y. Sung, I. D. Williams, H. S. Kwok and B. Z. Tang, *Adv. Funct. Mater.*, 2009, **19**, 905; (c) F. Mahtab, Y. Yu, J. W. Y. Lam, J. Z. Liu, B. Zhang, P. Lu, X. X. Zhang and B. Z. Tang, *Adv. Funct. Mater.*, 2011, **21**, 1733; (d) G. Yu, S. W. Yin, Y. Q. Liu, J.

5 S. Chen, X. J. Xu, X. B. Sun, D. G. Ma, X. W. Zhan, Q. Peng , Z. G. Shuai, B. Z. Tang, D. B. Zhu, W. H. Fang and Y. Luo, *J. Am. Chem. Soc.*, 2005, **127**, 6335.

5 J. Mei, N. L. C. Leung, R. T. K. Kwok, J. W. Y. Lam and B. Z. Tang, *Chem. Rev.*, 2015, **115**, 11718–11940.

6 R. Hu, J. L. Maldonado, M. Rodriguez, C. Deng, C. K. W. Jim, J. W. Y Lam, M. M. F. Yuen, G. Ramos-Ortiz and B. Z. Tang, *J. Mater. Chem.* 2012, **22**, 232–240.

7 J. Wang, J. Mei, W. Yuan, P. Lu, A. Qin, J. Sun, Y. Ma and B. Z. Tang, *J. Mater. Chem.* 2011, **21**, 4056–4059.

8 N. B. Shustova, B. D. McCarthy and M. Dincă, *J. Am. Chem. Soc.*, 2011, **133**, 20126–20129

9 (a) X. Sun, X. Liu, X. Xu, C. Yang, G. Yu, S. Chen, Z. Zhao, W. Qiu, Y. Li and D. Zhu, *J. Phys. Chem. B*, 2005, **109**, 10786; (b) Y. Shirota, *J. Mater. Chem.*, 2005, **15**, 75; (c) X. Y. Shen, W. Z. Yuan, Y. Liu, Q. Zhao, P. Lu, Y. Ma, I. D. Williams, A. Qin, J. Z. Sun and B. Z. Tang, *J. Phys. Chem. C*, 2012, **116**, 10541; (d) X. Y. Shen, Y. J. Wang, E. Zhao, W. Z. Yuan, Y. Liu, P. Lu, A. Qin, Y. Ma, J. Z. Sun and B. Z. Tang, *J. Phys. Chem. C*, 2013, **117**, 7334; (e) F. S. Kim, X. Guo, M. D. Watson and S. A. Jenekhe, *Adv. Mater.*, 2010, **22**, 478; (f) T. C. Lin, G. S. He and Q. Zheng, *J. Mater. Chem.*, 2006, **16**, 2490.

10 (a) E. Cariati, V. Lanzeni, E. Tordin, R. Ugo, C. Botta, A. Giacometti Schieroni, A. Sironi and D. Pasini, *Phys. Chem. Chem. Phys.*, 2011, **13**, 18005; (b) C. Coluccini, A.K. Sharma, M. Caricato, A. Sironi, E. Cariati, S. Righetto, E. Tordin, C. Botta, A. Forni, and D. Pasini, *Phys. Chem. Chem. Phys.*, 2013, **15**, 1666

11 T. Virgili, A. Forni, E. Cariati, D. Pasini and C. Botta, *J. Phys. Chem. C*, 2013, **117**, 27161.

12 M. M. Mróz, S. Benedini, A. Forni, C. Botta, D. Pasini, E. Cariati and T. Virgili, *Phys. Chem. Chem. Phys.*, 2016, DOI: 10.1039/c6cp02988d

13 C. Botta, S. Benedini, L. Carlucci, A. Forni, D. Marinotto, A. Nitti, D. Pasini, S. Righetto and E. Cariati, *J. Mater. Chem. C*, 2016, **4**, 2979-2989.

14 C. Hansch, A. Leo and R. W. Taft, *Chem. Rev.* 1991, **91**, 165-195

15 A. J. Zucchero, P. L. McGrier and U. H. F. Bunz, *Acc. Chem. Res.*, 2010, **43**, 397;

16 Y. M. Issa and W. H. Hegazy, *Synth. React. Inorg. Met-Org. Chem.*, 2000, **30**, 1731-1746.

17 O. Attanasi, P. Filippone and A. Mei, *Synth. Commun.*, 1983, **13**, 1203-1208

18 S. Zhu, B. Xu and J. Zhang, *J. Fluorine Chem.*, 1995, **74**, 167-170.

19 I. Shibuya, Y. Taguchi, T. Tsuchiya, A. Oishi and E. Katoh, *Bull. Chem Soc Jpn*, 1994, **67**, 3048-3052

20 B. A. Burkett, J. M. Kane-Barber, R. J. O'Reilly and L. Shi, *Tetrahedron Lett.*, 2007, **48**, 5355-5358.

21 The free energy barrier for the dynamic process ($\Delta G_c^{\ddagger}$) could be calculated using the coalescence method, where values for the rate constant k_c, at the coalescence temperature (T_c) were calculated from the approximate expression $k_c = \pi(\Delta \nu)/2^{0.5}$, where $\Delta \nu$ is the limiting chemical shift difference (Hz) between the coalescing signals in the absence of exchange, The Eyring equation was subsequently employed. See: a) I. 0. Sutherland, *Annu. Rep. NMR Spectrosc.* 1971, 4, 71-235. See also: b) P.R. Ashton, S. E. Boyd, S. Menzer, D. Pasini, F. M. Raymo, N. Spencer, J.F. Stoddart, A. J. P. White, D. J. Williams and P.G. Wyatt, *Chem. Eur. J.* 1998, **4**, 299-310.

22 a) M. Yu. Antipin, T. V. Timofeeva, R. D. Clark, V. N. Nesterov, M. Sanghadasa, T. A. Barr, B. Penn, L. Romero and M. Romero, *J. Phys. Chem. A* 1998, **102**, 7222-7232; b) K. Wang, Z. Wang and C. Yan, *Acta Cryst.* 2001, **E57**, o214-o215; c) R. D. Gandour and F. R. Fronczek, CSD Communication (Private Communication), 2015; (d) V. K. Gupta and R. A. Singh, *RSC Adv.* 2015, **5**, 38591–38600.

23 a) W. Ma, S.-Y Zhang, J.-Y. Wu, Y.-P. Tian and H.-K. Fun, *Chin. J. Appl. Chem.*, 2003, 20, 862. b) Y. Jing and L.-T. Yu, *Acta Cryst.* 2011, **E67**, o1556.

24 F. H. Allen, O. Kennard, D. G. Watson, L. Brammer, A. G. Orpen and R. Taylor, *J. Chem. Soc., Perkin Trans. 2*, 1987, S1.

25 N. F. Phelan and M. Orchin, *J. Chem. Educ.* 1968, **45**, 633.

26 M. H. Habibi, K. Barati, H. Etedali Habibadi, R. W. Harrington and W. Clegg, *Anal. Sci.*, 2008, **24**, x285-x286.

27 E. Solcaniova, P. Hrnciar and T. Liptaj, *Org. Magn. Res.*, 1982, **18**, Pages55-7,

28 J. S. Yadav, D. C. Bhunia, V. K. Singh and P. Srihari, *Tetrahedron Lett.*, 2009, **50**, 2470–2473

29 A. Szłap, S. Kula, U. Błaszkiewicz, M. Grucela, E. Schab-Balcerzak and M. Filapek, *Dyes and Pigments*, 2016, **129**, 80-89.

30 G. B. Kharas, S. M. Russell, V. Tran, Q. L. Tolefree, D. M. Tulewicz, A. Gora, J. Bajgoric, M. T. Balco, G. A. Dickey and G. Kladis, *J. Macromol. Sci. Part A-Pure Appl. Chem.*, 2008, **45**, 5-8.

31 J. S. A. Brunskill, A. De and G. M. Vas, *Synth. Commun.*, 1978Volume8 Pages1-7

32 US Patent No. 20030000130

33 G. Charles, *Bull. Soc. Chim. Fr.*, 1963, **8-9**, 1559-65.

34 J. Moreau, U. Giovanella, J.-P. Bombenger, W. Porzio, V. Vohra, L. Spadacini, G. Di Silvestro, L. Barba, G. Arrighetti, S. Destri, M. Pasini, M. Saba, F. Quochi, A. Mura, G. Bongiovanni, M. Fiorini, M. Uslenghi and C. Botta, *ChemPhysChem* 2009, **10**, 647.

35 SMART, SAINT and SADABS, Bruker AXS Inc., Madison, Wisconsin, USA, 1997.

36 G. M. Sheldrick, *Acta Cryst.* 2008, **A64**, 112-122.

37 L. J. Farrugia, *J. Appl. Crystallogr.* 2012, **45**, 849-854.

38 A. C. T. North, D. C. Phillips, F. S. Mathews, *Acta. Crystallogr.* 1968, **A24**, 351-359.

39 A. Altomare, M. C. Burla, M. Camalli, G. L. Cascarano, C. Giacovazzo, A. Guagliardi, A. G. G. Moliterni, G. Polidori and R. Spagna, *J. Appl. Crystallogr.* 1999, **32**, 115-119.

Supporting Information for:

Structure-Activity Relationships for the Solid State Emission of a New Family of "Push-Pull" π-Extended Chromophores

Andrea Nitti,[a] Francesca Villafiorita-Monteleone,[b] Aurora Pacini,[a] Chiara Botta,[b] Tersilla Virgili,[c] Alessandra Forni,[d] Elena Cariati,[e] Massimo Boiocchi,[f] and Dario Pasini[*,a]

a.   *Department of Chemistry and INSTM Research Unit, University of Pavia, Viale Taramelli, 10, 27100 Pavia, Italy. Email: dario.pasini@unipv.it.*

b.   *ISMAC -CNR, Via Corti 12, 20133 Milano, Italy*

c.   *IFN-CNR, Dipartimento di Fisica, Politecnico di Milano, Piazza Leonardo Da Vinci, 32, 20132 Milano, Italy*

d.   *ISTM - CNR, c/o Dipartimento di Chimica, Università degli Studi di Milano, Via Venezian, 21, 20133 Milano, Italy*

e.   *Università degli Studi di Milano, Dipartimento di Chimica, via Golgi 19, 20133 Milano, Italy*

f.   *Centro Grandi Strumenti, University of Pavia, Via Bassi, 21 - 27100 - Pavia, Italy*

Table of Contents:
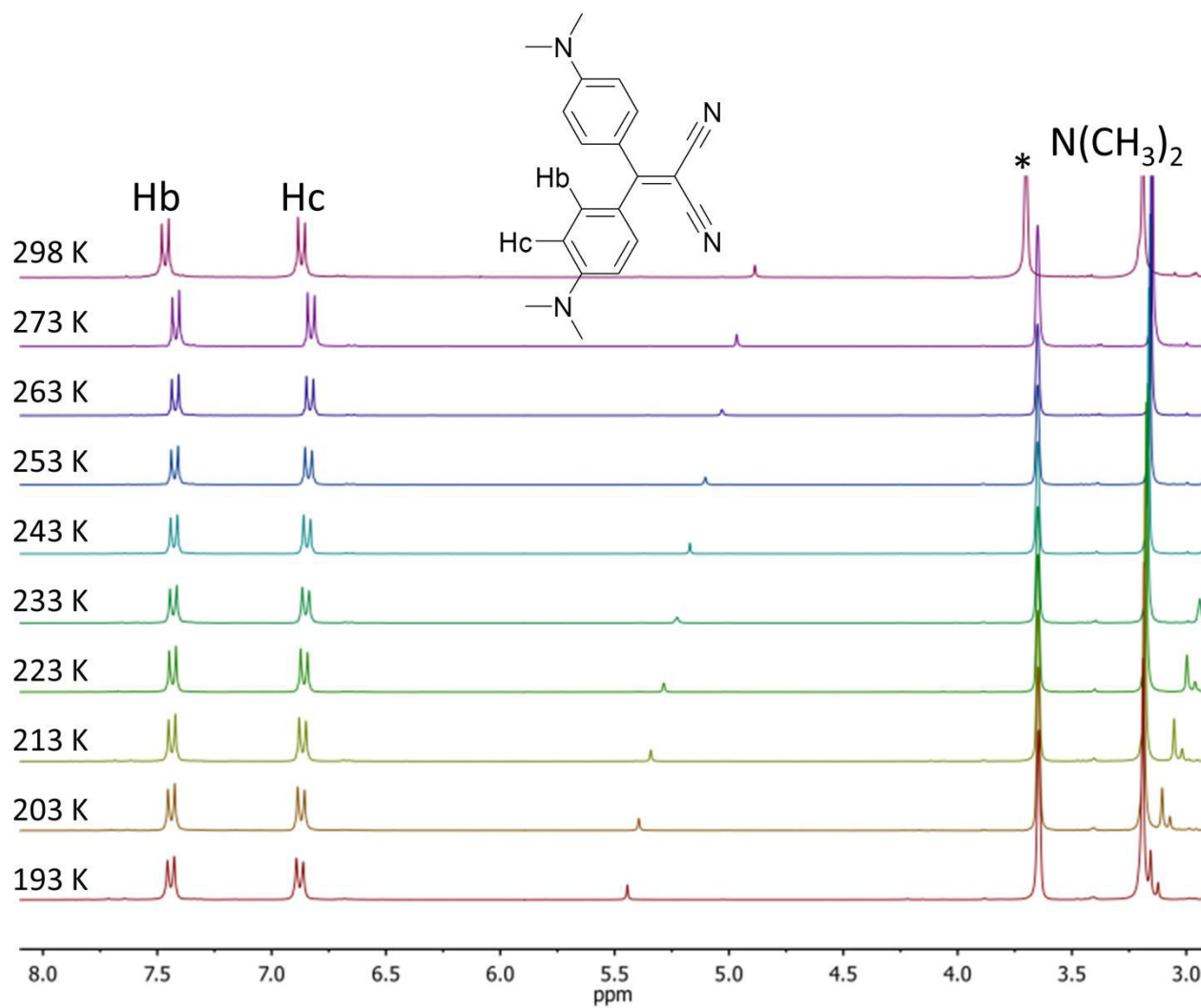
Fig. S1. Variable Temperature ^{1}H NMR spectra (300 MHz, d_8-THF) of compound **5a**. The asterisk denotes residual solvent peak.

Table S1. ^{1}H-NMR (200 MHz, CDCl$_3$, 298 K) chemical shifts of compounds **2** and **3**.

Compound	t, CH$_3$	m, CH$_2$	s, COCH$_3$	s,N(CH$_3$)$_2$	t, CH$_2$	q, CH$_2$	s, OCH$_3$	d, ArH	s, Vinyl CH
2a	--	--	2.39 2.37	3.05	--	--	--	6.65 7.31	7.40
2b	--	--	--	3.14	--	--	--	6.67 7.35	7.86
2c	--	--	2.12	--	--	--	3.83	6.93 7.47	7.63
2d	--	--	--	--	--	--	3.87	6.97 7.42	7.99
2e	1.25	--	--	--	--	3.48	--	6.65 7.34	7.83
2f	--	2.04	2.37 2.38	--	3.36	--	--	6.52 7.30	7.40
2g	--	2.08	--	--	3.45	--	--	6.45 7.35	7.85
3a	--	--	--	3.15	--	--	--	6.68 7.83	7.48
3b	1.25	--	--	--	--	3.48	--	6.68 7.81	7.44
3c	--	2.09	--	--	3.45	--	--	6.57 7.80	7.44

Table S2. ^{13}C-NMR (75 MHz, CDCl$_3$, 298 K) chemical shifts of selected compounds **2** and **3**.

Compound	CH$_3$	CH$_2$	(CH$_3$)N	C$_q$	ArCH	C$_q$-CN	C$_q$-CF$_3$	C$_q$	VinylCH	C$_q$-CO
2a	26.1 31.6	--	40.0	137.8	111.8 132.2	--	--	120.1 151.8	140.9	207.0 196.3
2b	--	--	39.9	118.2	111.9 134.9	--	115.3 117.1	119.8 154.2	152.0	187.6 177.5
2f	26.1 31.6	47.4 25.3	--	137.1	111.7 132.4	--	--	119.3 149.4	141.3	207.2 196.1
2g	--	25.2 47.8	--	118.1	112.4 135.2	--	115.3 117.1	119.2 152.1	151.8	187.6 177.5
3a	--	--	40.0	71.9	111.5 133.7	114.8 115.9	--	119.2 154.1	157.9	--
3b	12.4	44.8	--	71.0	111.2 134.0	114.9 116.1	--	118.8 152.3	157.7	--
3c	--	25.2 47.8	--	70.9	111.9 133.9	115.1 116.1	--	119.0 151.8	157.9	--

Table S3. ^{1}H-NMR (200 MHz, CDCl$_3$, 298 K) chemical shifts of compounds **4** and **5**.

Compound	s, CH_3	s, N(CH_3)$_2$	s, OCH_3	s, ArOCH_3	d, ArH
4a	--	2.85	3.76	--	6.54 7.12
4b	1.92	3.03	--	--	6.65 7.07
4c	--	3.01	3.62	--	6.63 7.08
4d	--	--	3.83	3.63	6.84 7.12
4e	1.93	--	--	3.84	6.88 7.12
4f	1.93	--	3.88	3.61	6.86 7.12
5a	--	3.08	--	--	6.69 7.41
5b	--	--	--	3.89	6.98 7.43

Table S4. ^{13}C-NMR (75 MHz, CDCl$_3$, 298 K) chemical shifts of selected compounds **4** and **5**.

Compound	CH$_3$	N(CH$_3$)$_2$	OCH$_3$	ArOCH$_3$	C$_q$	ArCH	C$_q$-2CN	C$_q$	C$_q$-COMe	C$_q$-COOMe
4b	31.1	40.1		--	126.3 154.7	111.4 127.4	--	132.5 151.6	204.5	--
4c	30.2	40.0	51.7	--	127.1 156.9	111.1 131.6	--	132.6 151.7	201.6	169.5
4d	--	40.1	51.8	--	118.8 158.9	111.6 127.9	--	131.5 151.0	--	168.0
4e	31.1	--	--	55.3	141.3 161.1	113.9 131.9	--	150.3 161.8	204.0	--
4f	30.3	--	51.9	55.3	131.8 153.6	113.9 131.9	--	132.4 160.7	201.3	168.2
5a	--	39.9	--	--	69.1 173.8	110.0 123.0	117.2	133.5 153.1	--	--
5b	--	--	--	55.5	77.4 173.8	114.1 132.9	114.9	128.3 163.3	--	--

S4

Optical Properties
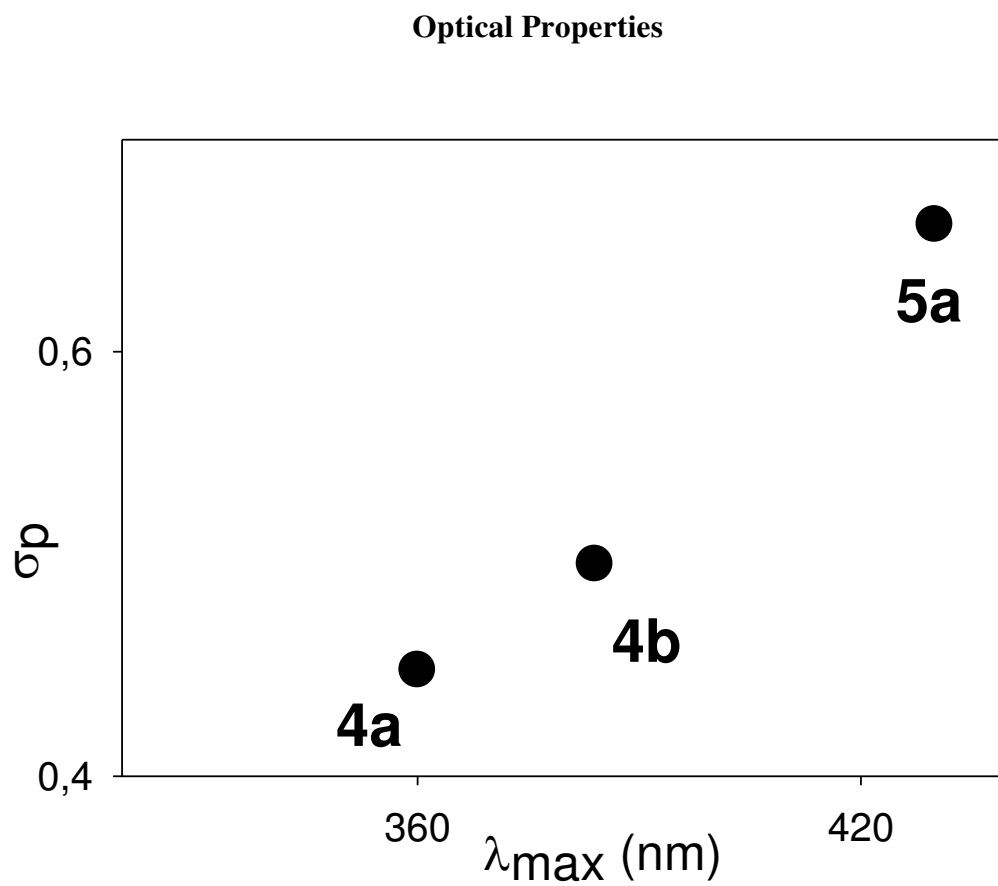
Figure S2. Correlation between λ_{max} and σ_p Hammett's parameters for dimethylamino-terminated compounds **4** and **5** (fitting coefficient $r^2 = 0,99$).
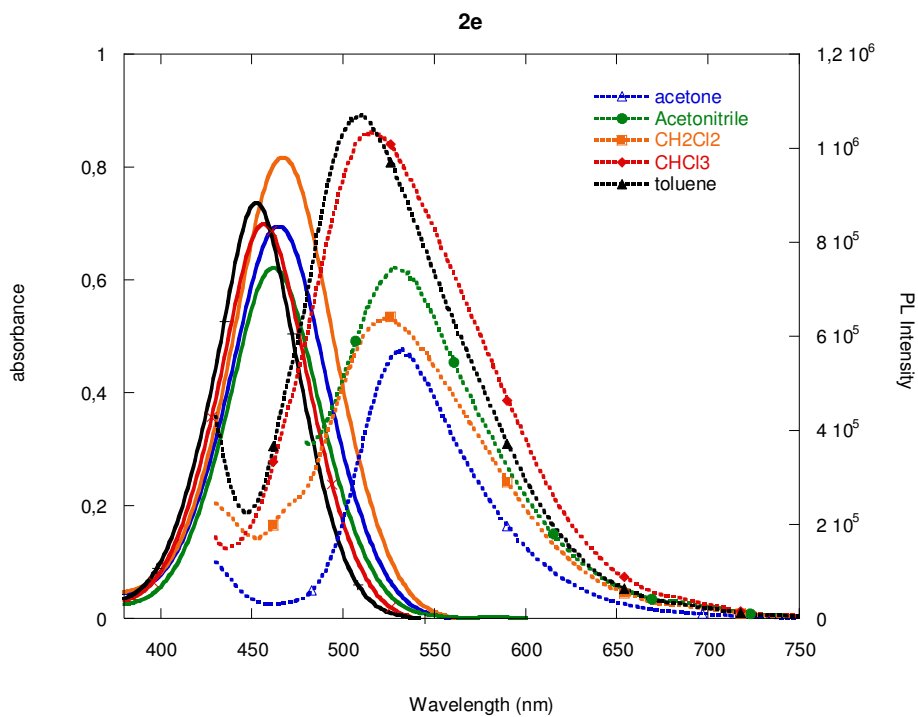
Figure S3. Solvatochromism of compound **2e**.
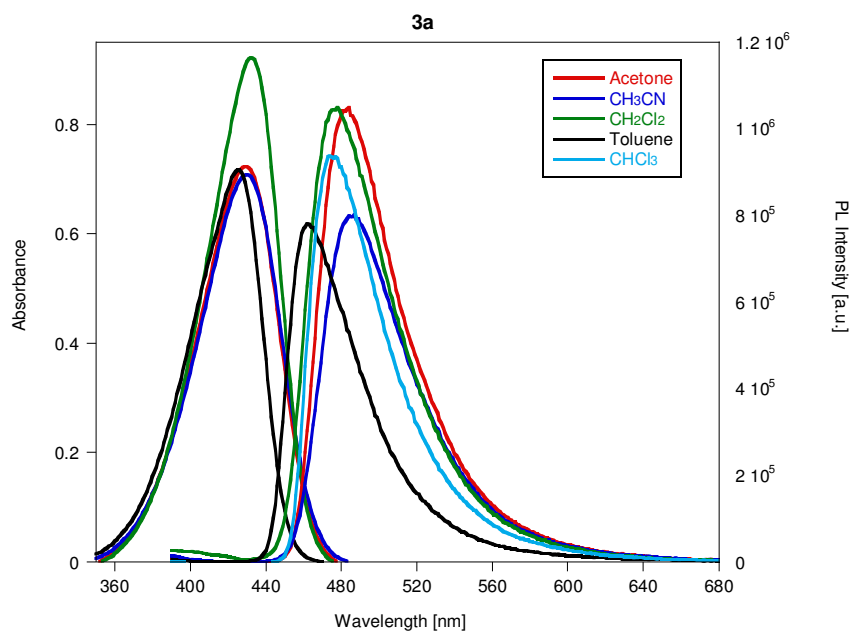
Figure S4. Solvatochromism of compound **3a**.
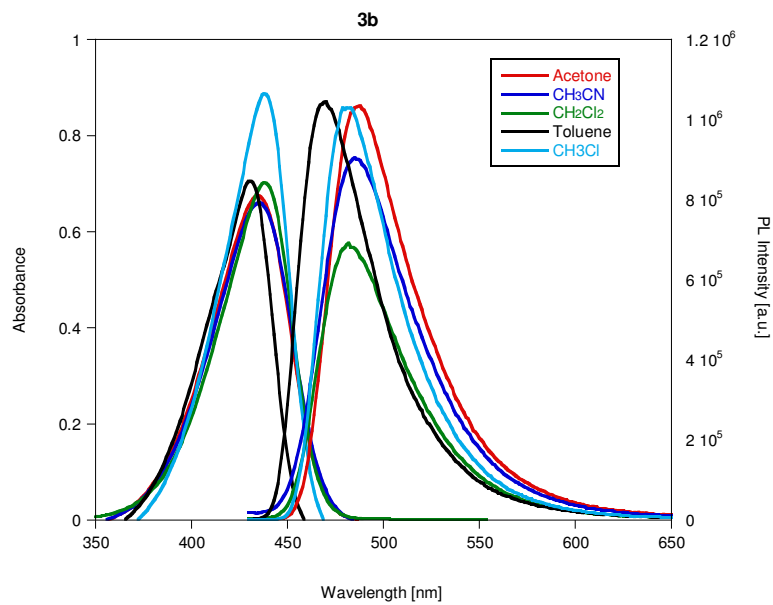
Figure S5. Solvatochromism of compound **3b**
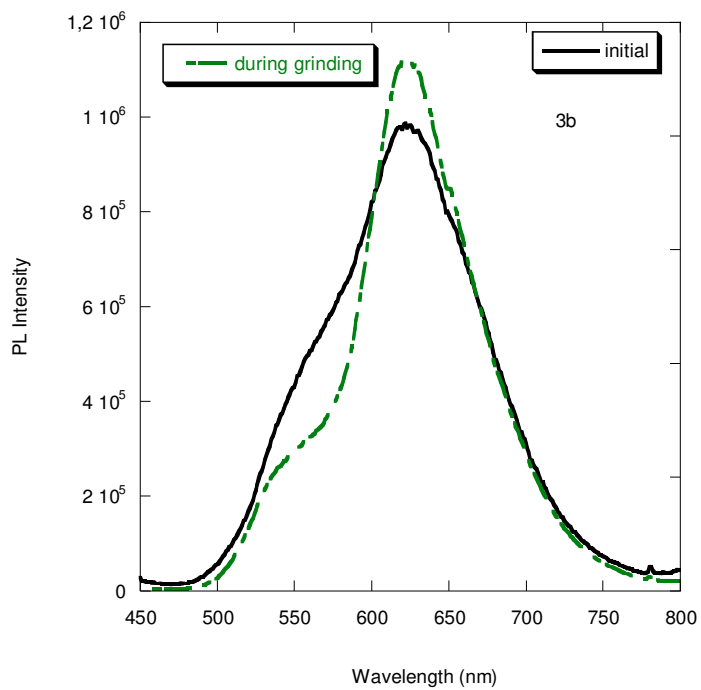
Figure S6. PL spectra of **3b** powders upon grinding

Copies of NMR and Mass Spectra of Newly Synthesized Compounds

Compound **2a**.

^{1}H NMR (CDCl$_3$, 200 MHz)
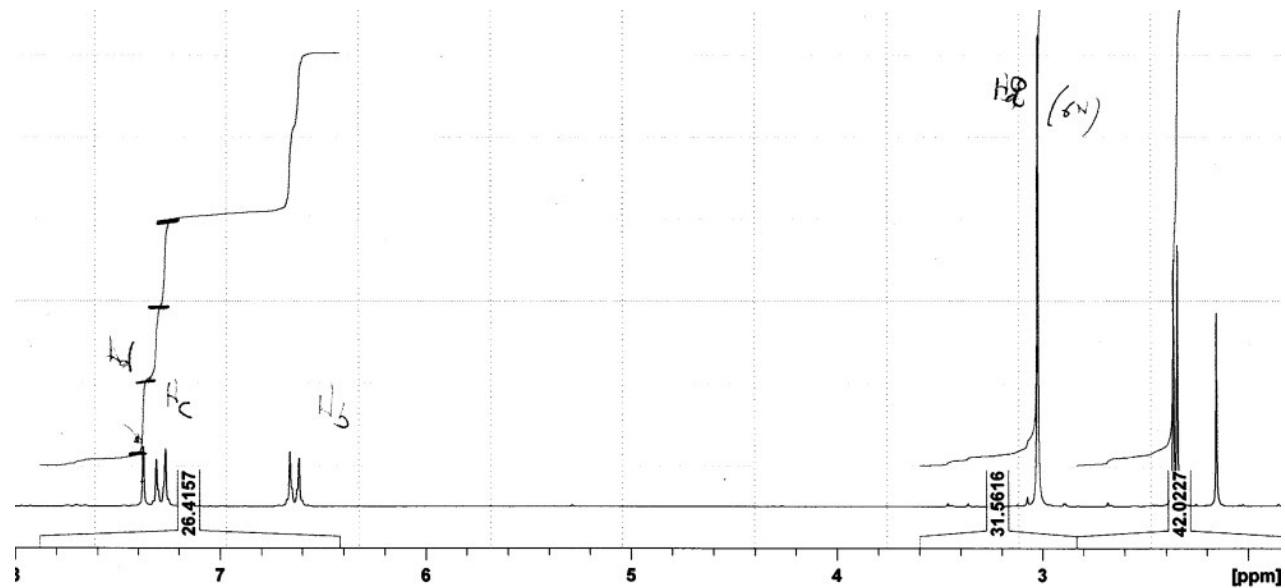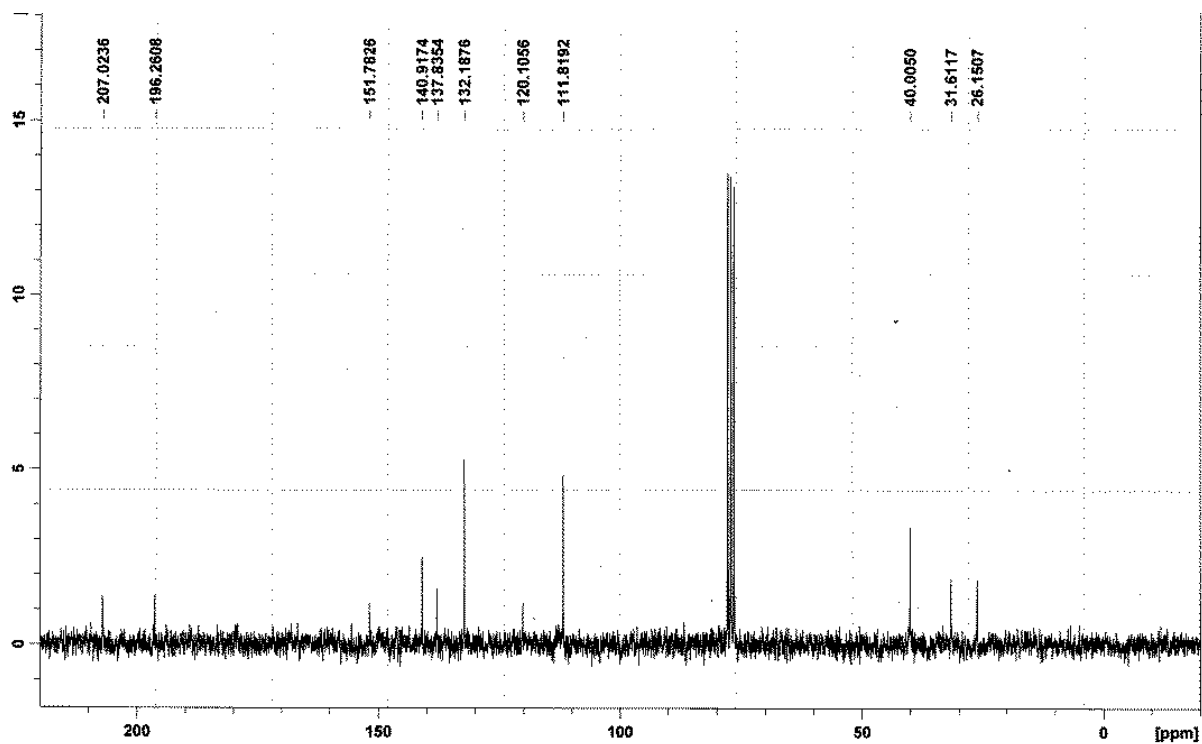
^{13}C NMR (CDCl$_3$, 75 MHz)

ESI-Mass spectrum
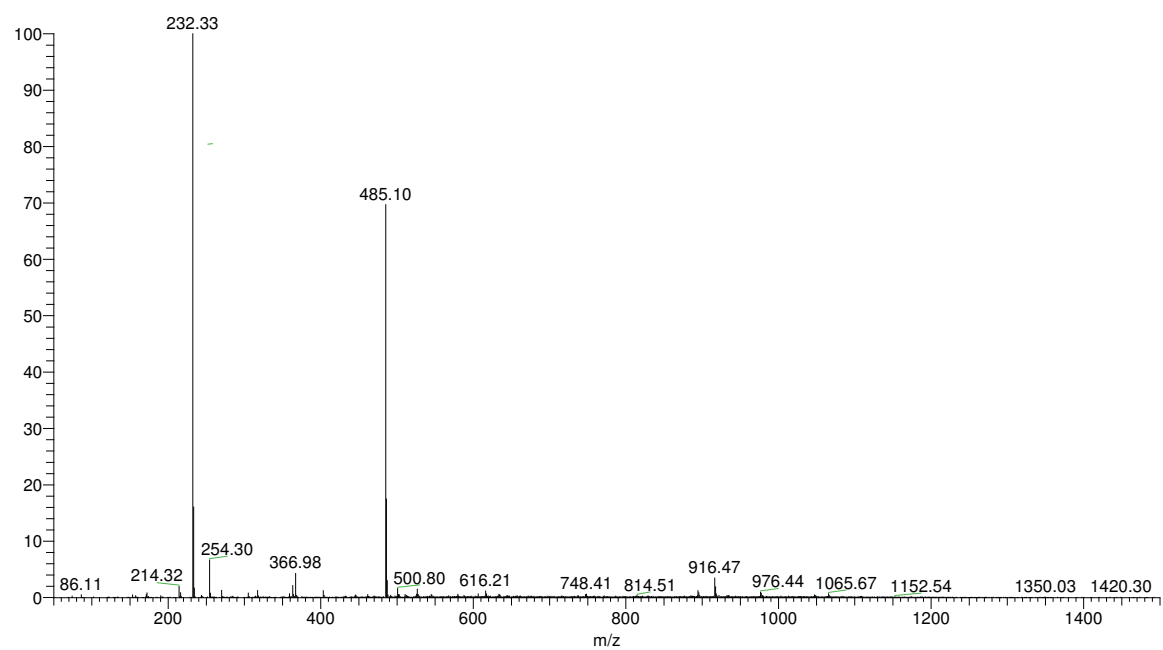
Compound **2c**.
^{1}H NMR (CDCl$_3$, 200 MHz)
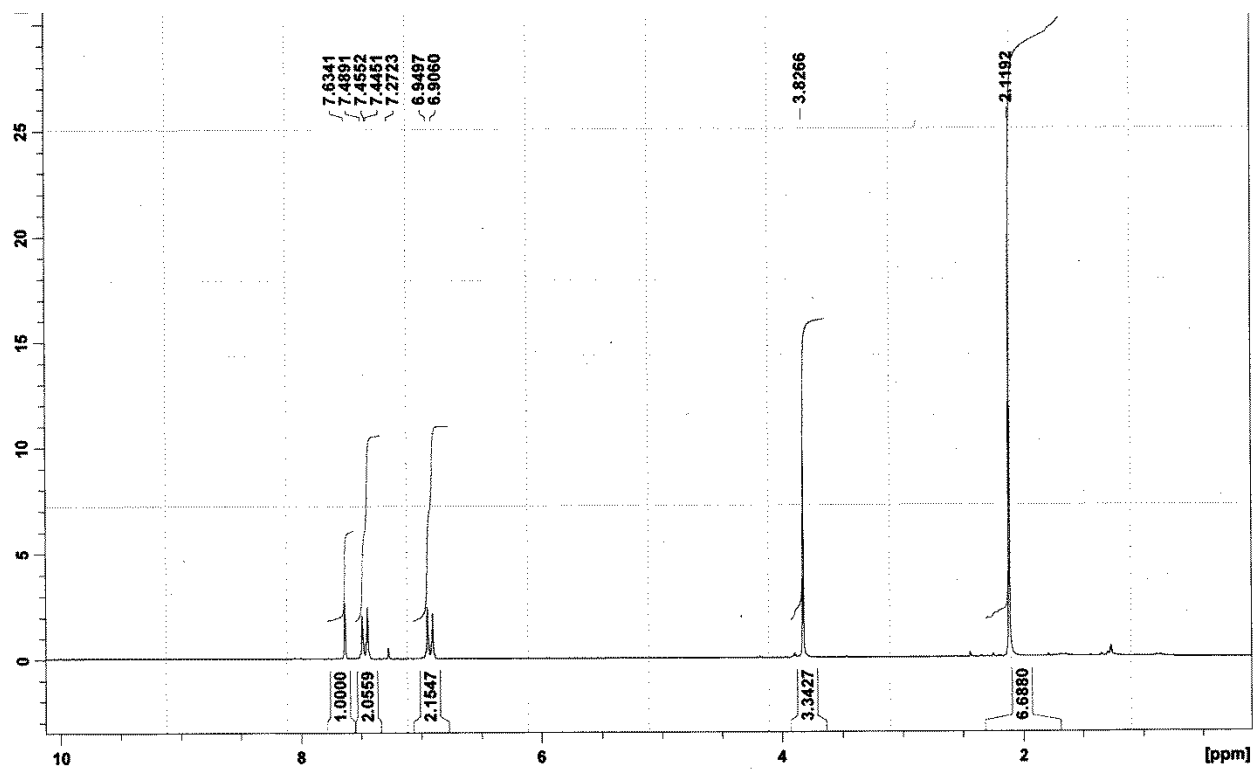
Compound **2d**.
^{1}H NMR (CDCl$_3$, 200 MHz)

S10
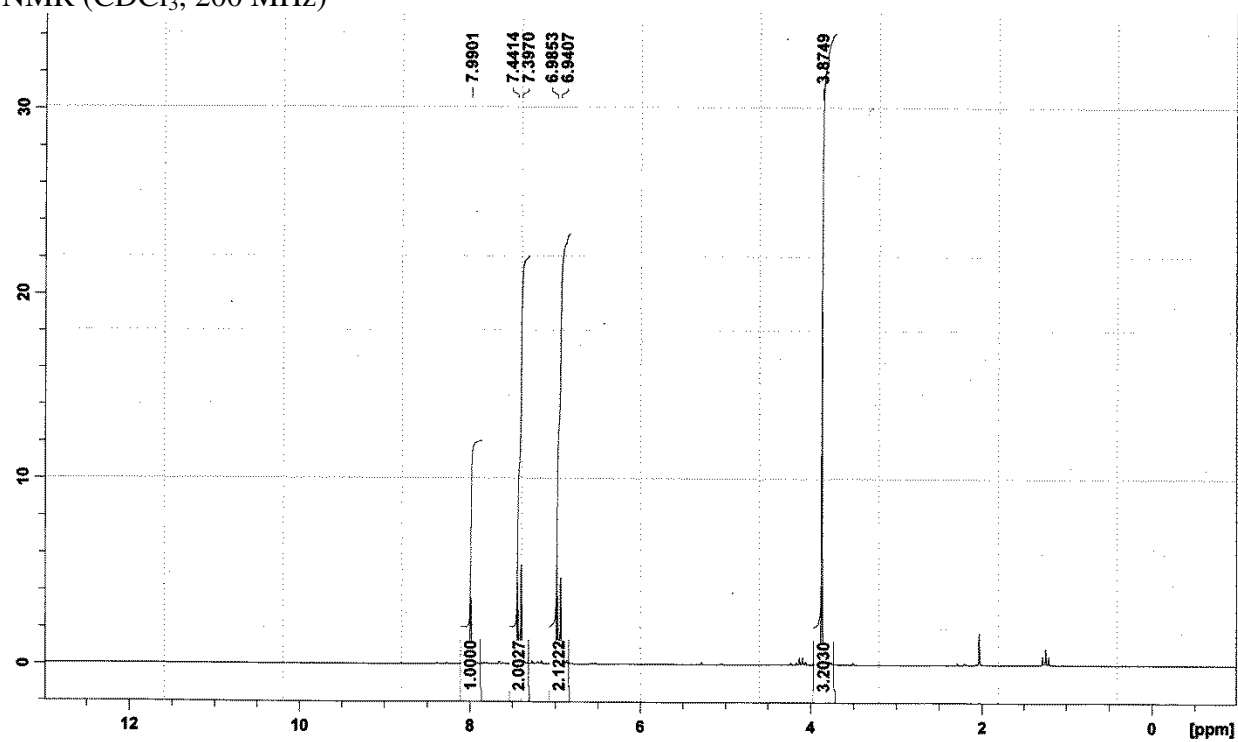
Compound **2e**.
^{1}H NMR (CDCl$_3$, 200 MHz)
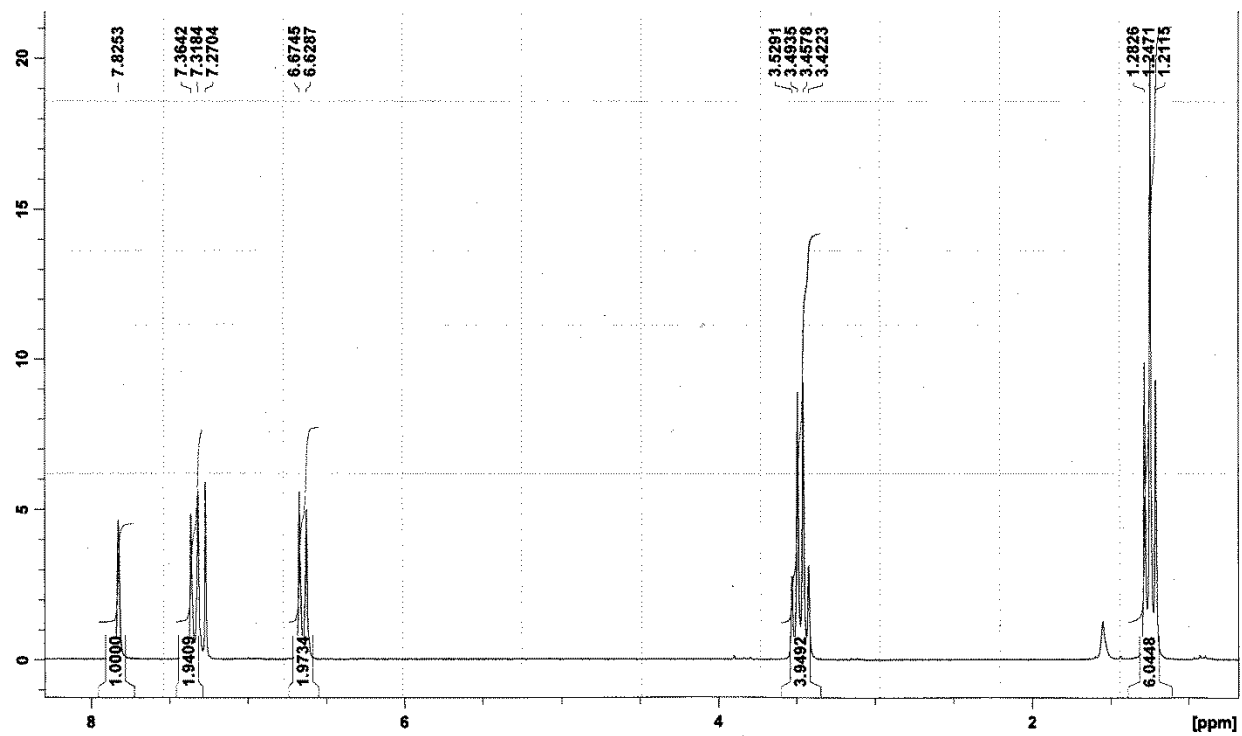
Compound **2f**.
^{1}H NMR (CDCl$_3$, 300 MHz)
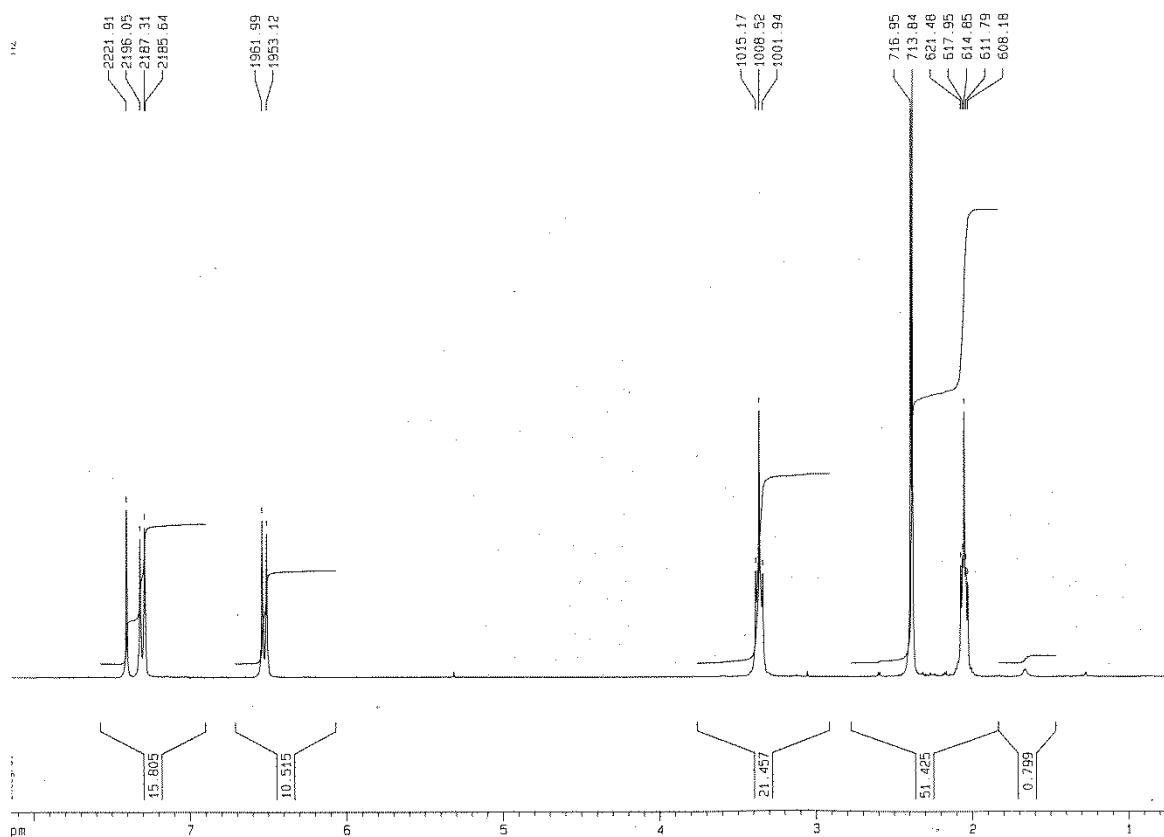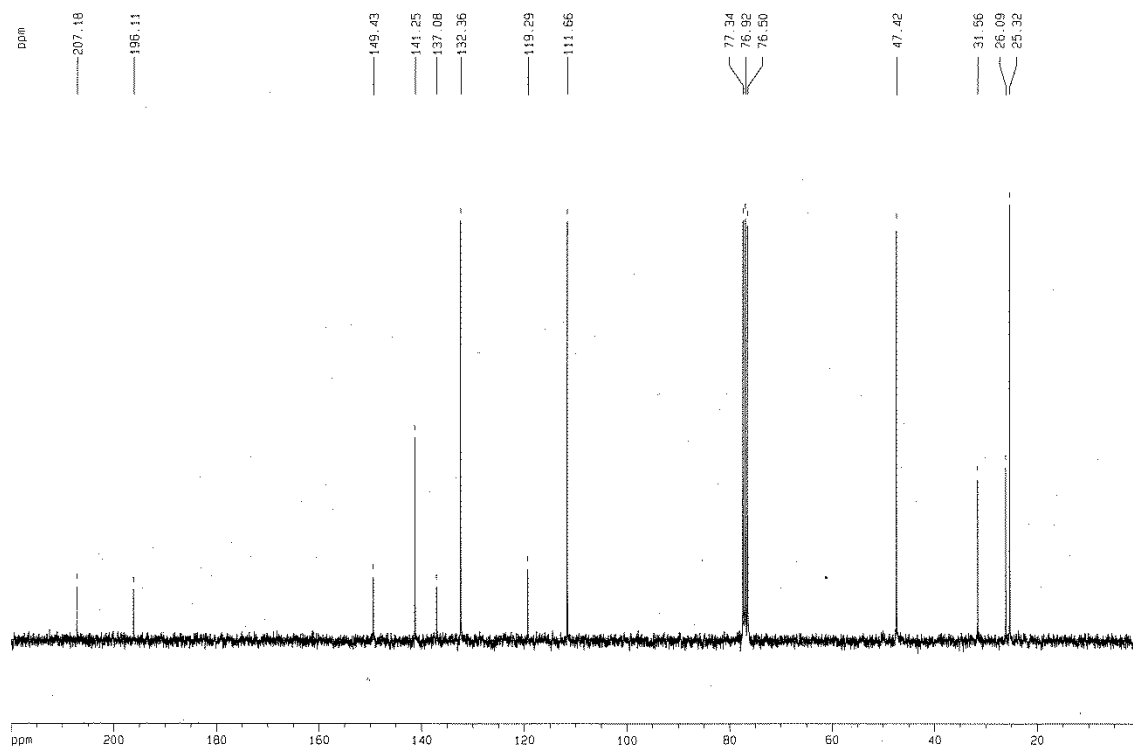
^{13}C NMR (CDCl$_3$, 75 MHz)

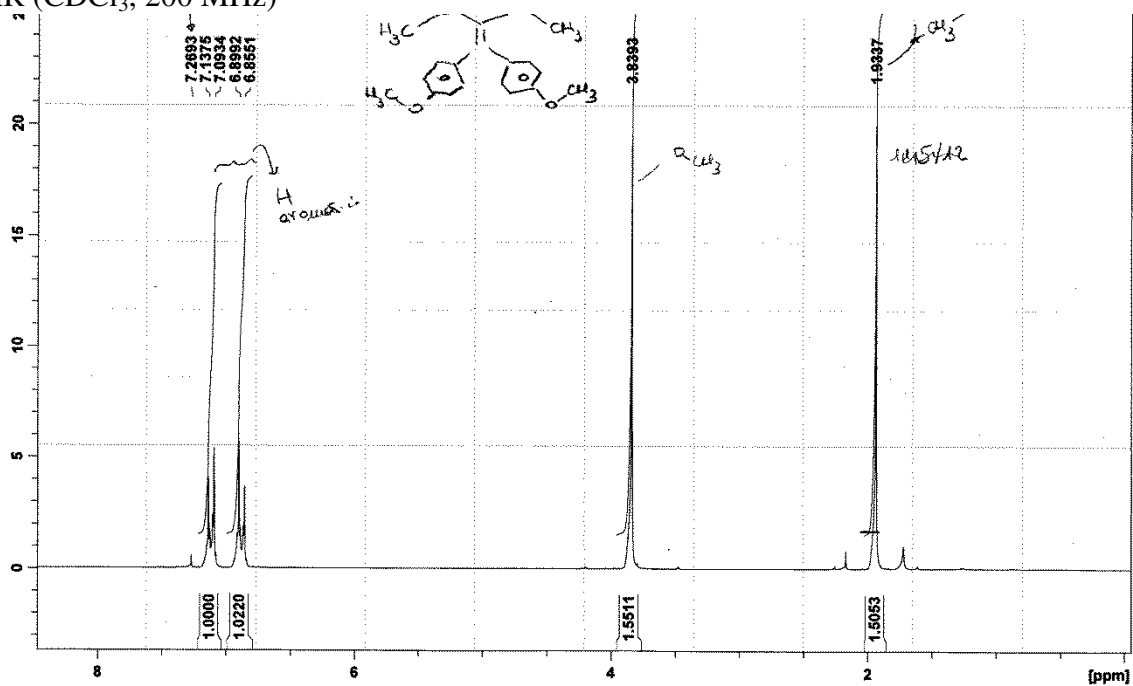^{13}C NMR DEPT (CDCl$_3$, 75 MHz)
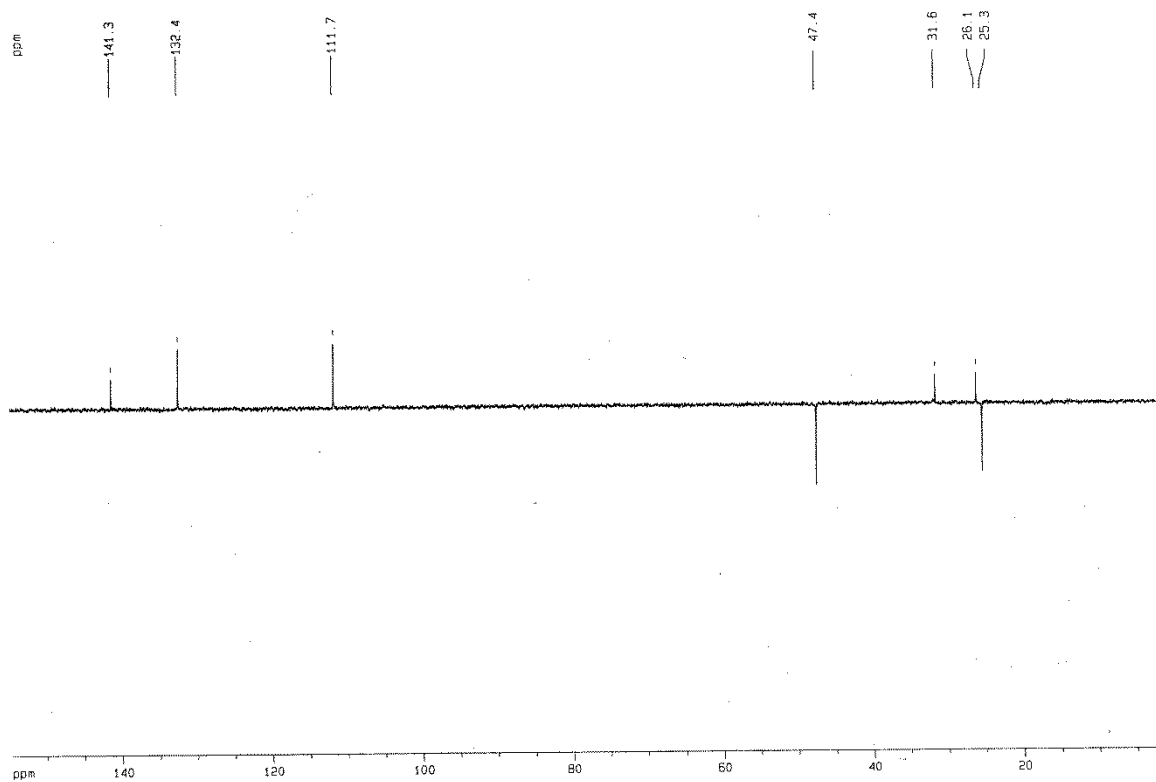
Compound **2g**.
^{1}H NMR (CDCl$_3$, 300 MHz)

Hz — 2358.51 — 2211.22 / 2202.18 — 1973.40 / 1964.37 — 1041.44 / 1034.76 / 1028.20 — 535.02 / 531.42 / 628.37 / 625.40 / 621.73

Integral: 7.311 | 15.001 | 15.124 | 30.626 | 29.254 | 2.685

ppm 8 7 6 5 4 3 2 1

^{13}C NMR (CDCl$_3$, 75 MHz)

152.10 / 151.88 — 135.16 — 119.20 / 118.10 — 112.38 — 77.33 / 76.91 / 76.49 — 47.79 — 25.18

180 160 140 120 100 80 60 40 20
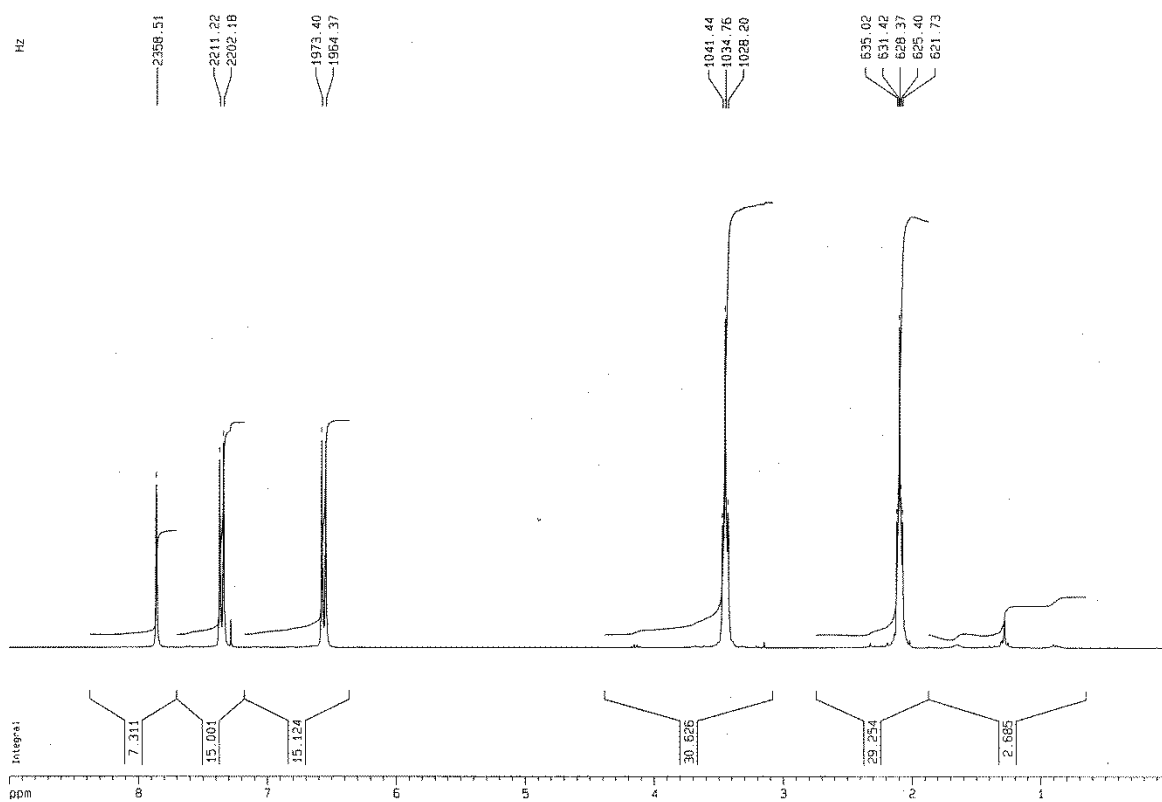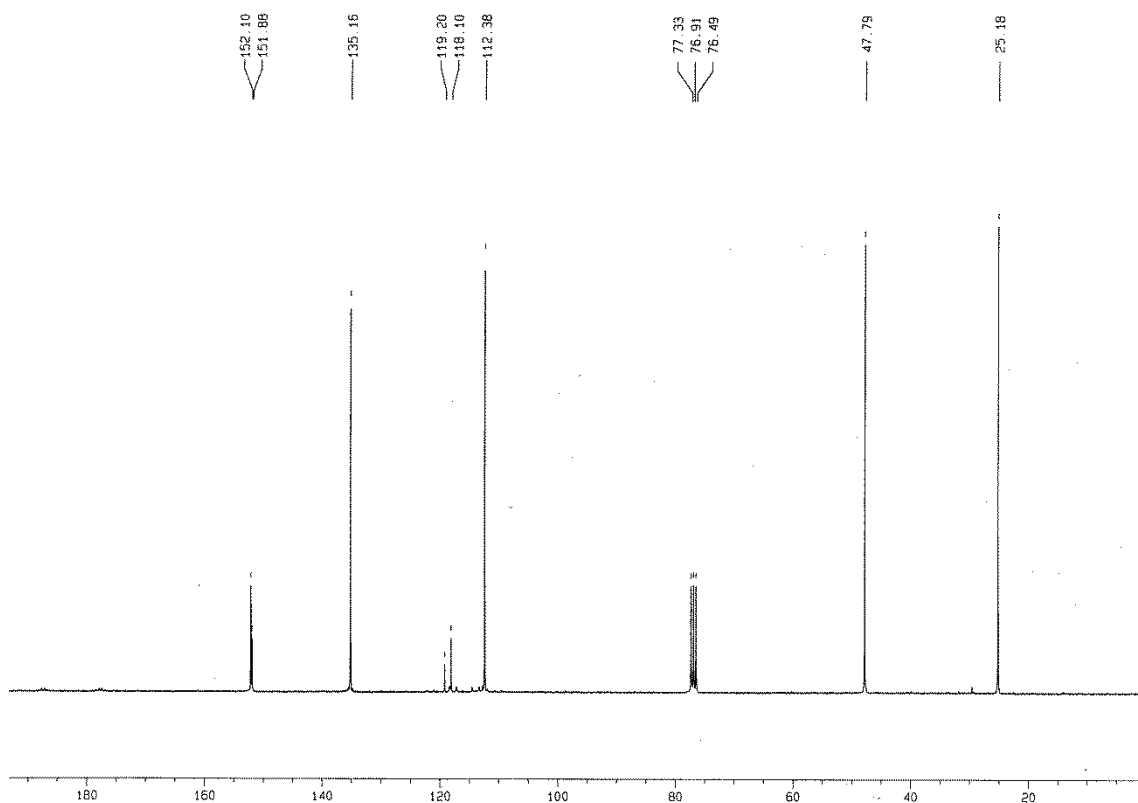
^{13}C NMR enlargement (CDCl$_3$, 75 MHz)
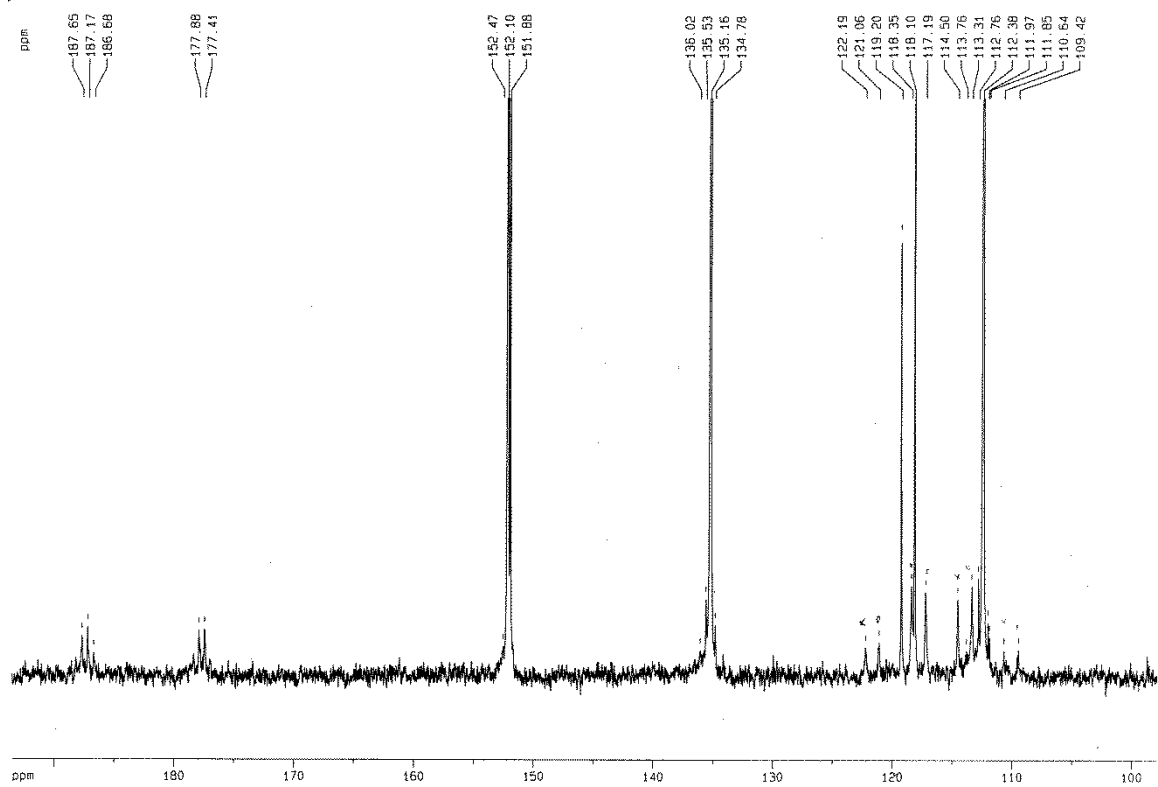
Compound **3a**.
^{1}H NMR (CDCl$_3$, 300 MHz)

2354.63
2345.50
2243.68
2185.73
2018.47
2009.31
949.26

24.850
2.017
17.467
52.207
3.439

8   7   6   5   4   3   2   1

^{13}C NMR (CDCl$_3$, 75 MHz)

ppm
157.98
154.12
133.68
119.20
115.85
114.79
111.49
77.33
77.12
76.91
76.49
71.89
39.97

180   160   140   120   100   80   60   40   20

Compound **3b**.
^{1}H NMR (CDCl$_3$, 300 MHz)

^{13}C NMR (CDCl$_3$, 75 MHz)

Compound **3c**.
^{1}H NMR (CDCl$_3$, 300 MHz)

Hz

2349.46
2340.49
2234.34
2185.55
1980.54
1971.45
1045.67
1038.95
1032.29
638.13
634.46
631.44
628.45
624.70
618.83
475.49
382.90

Integral

22.398
14.764
28.785
34.052

^{13}C NMR (CDCl$_3$, 75 MHz)

ppm

157.93
151.81
133.86
119.03
116.11
115.05
111.97
77.34
77.12
76.91
76.49
70.85
47.77
25.23

S18

Compound **4a**.
¹H NMR (CDCl₃, 200 MHz)
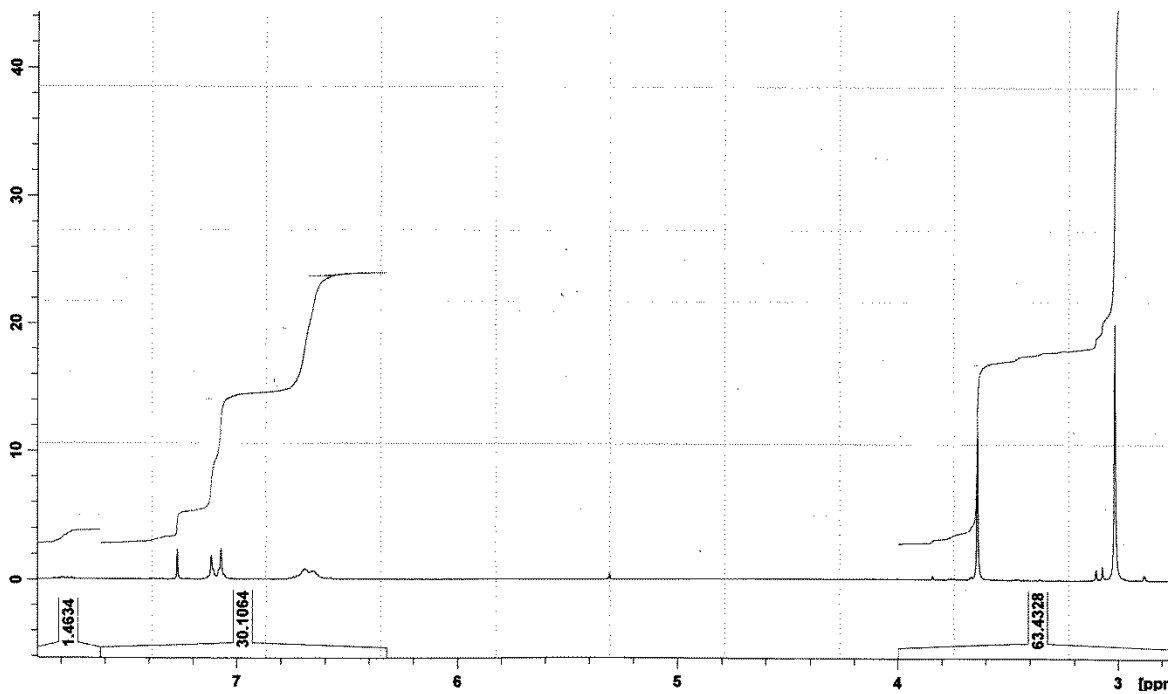
¹³C NMR (CDCl₃, 50 MHz)
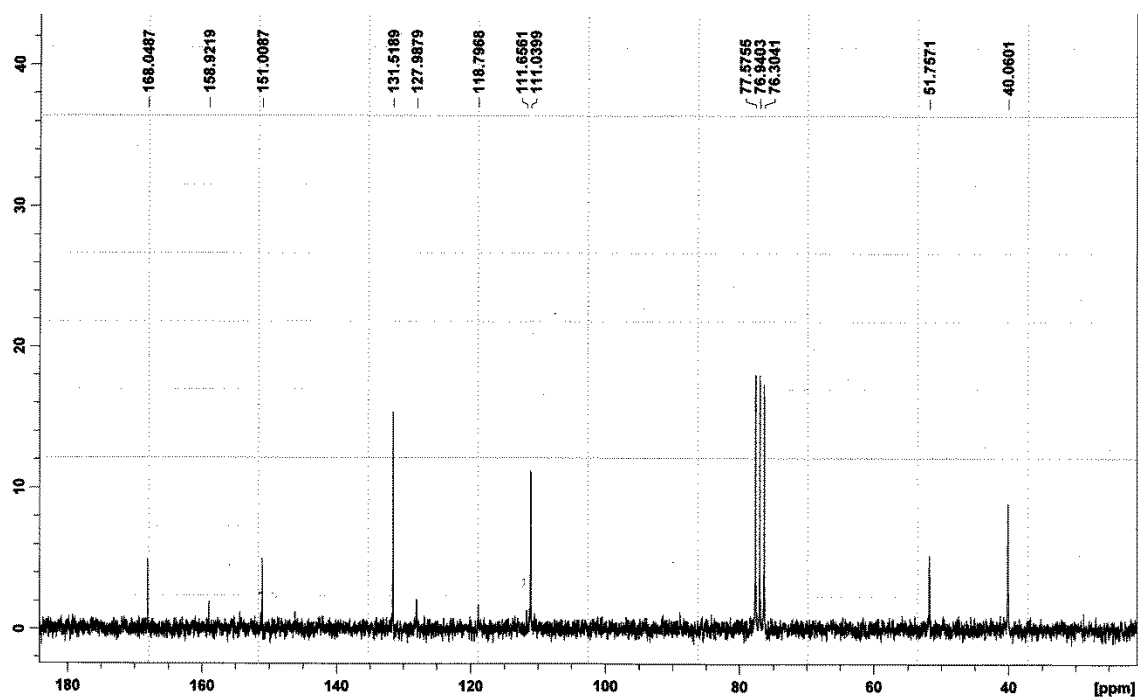
Compound **4b**.
^{1}H NMR (CDCl$_3$, 200 MHz)
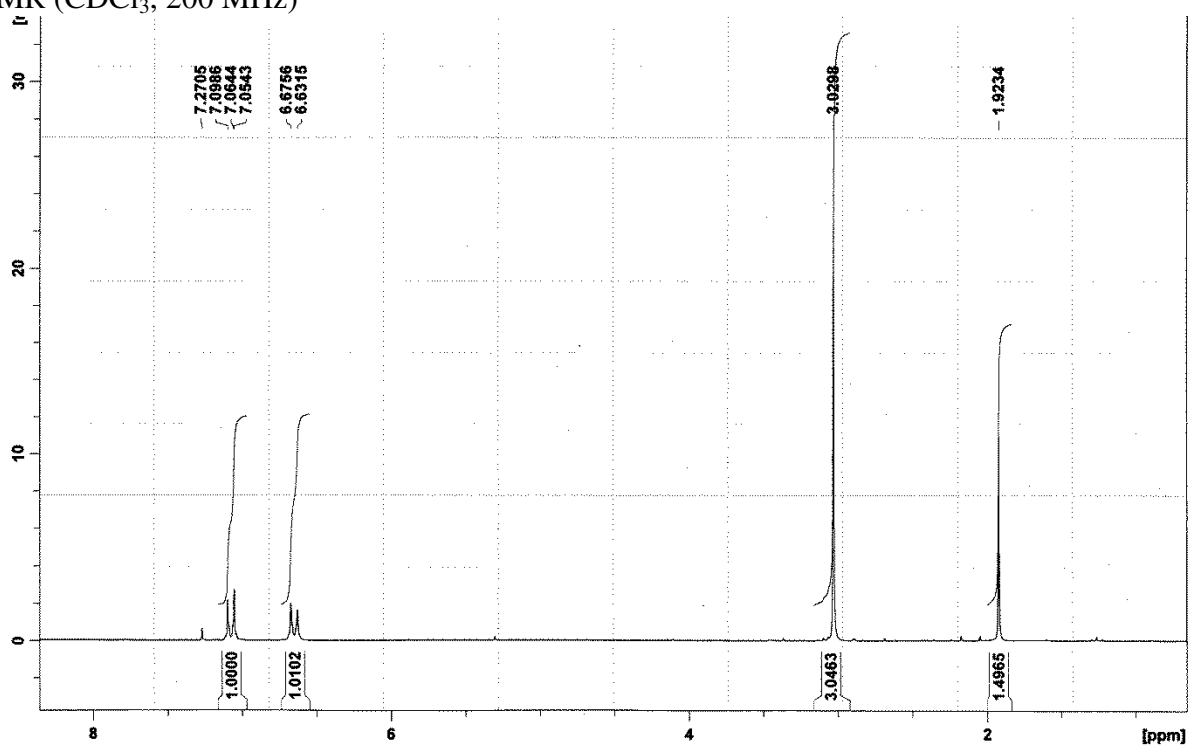
ESI-Mass spectrum
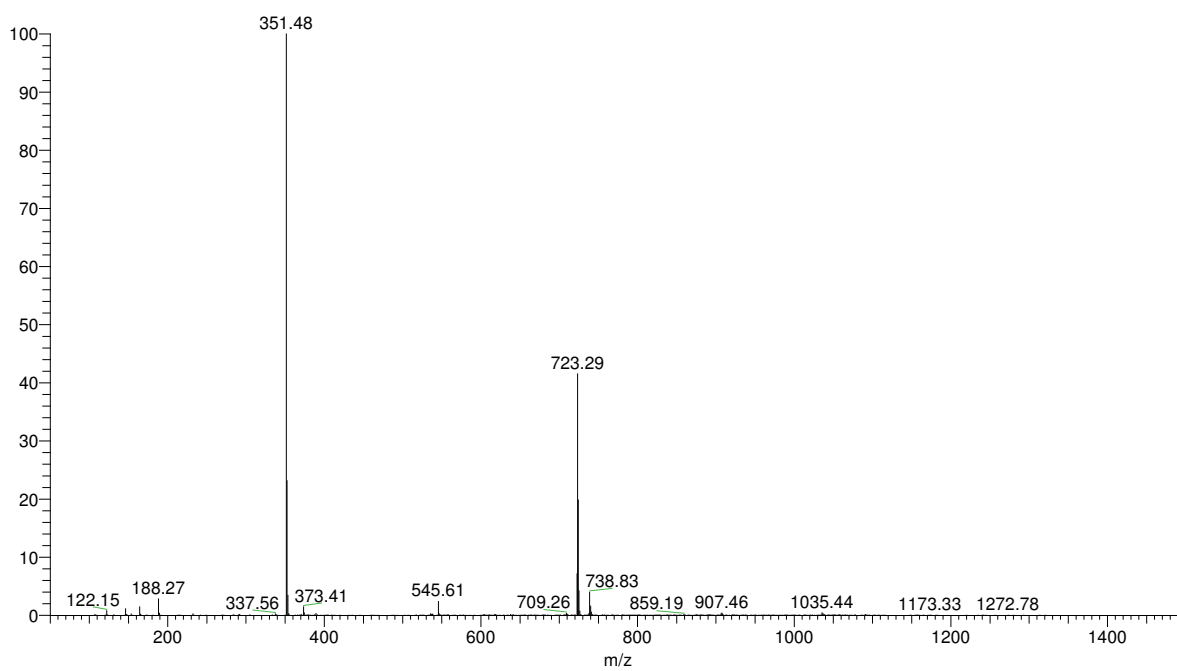
Compound **4c**.
^{1}H NMR (CDCl$_3$, 300 MHz)
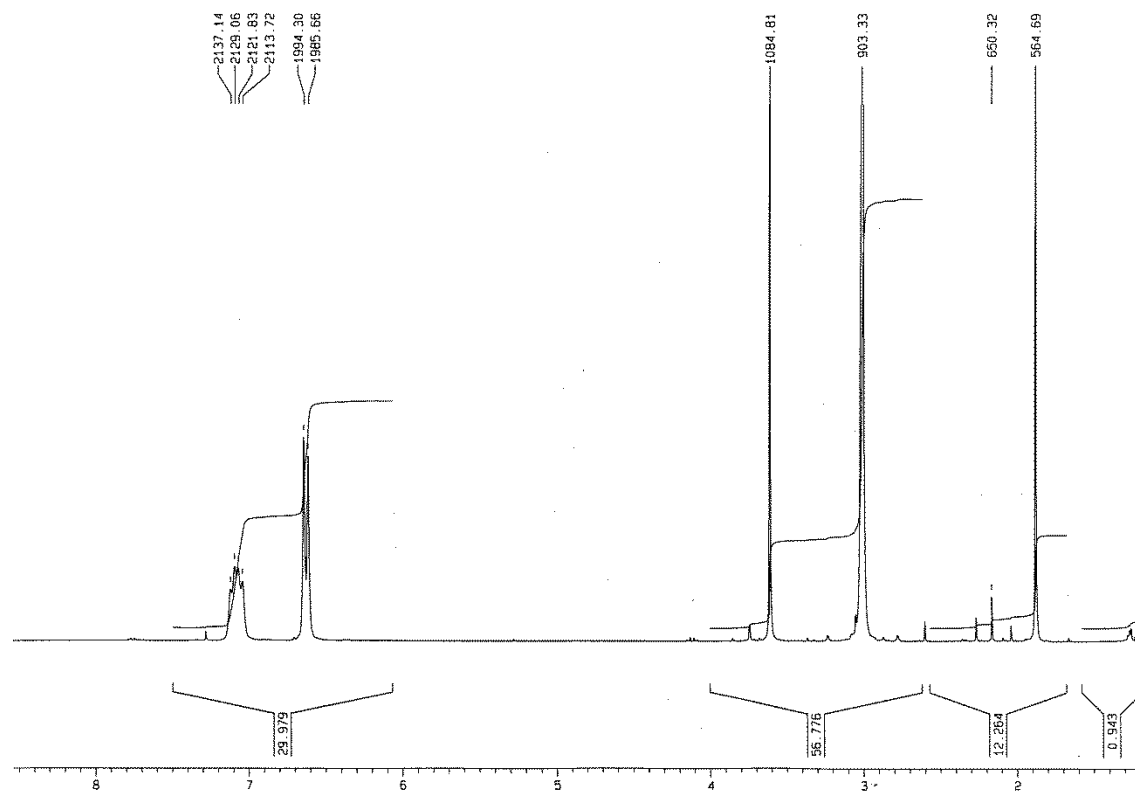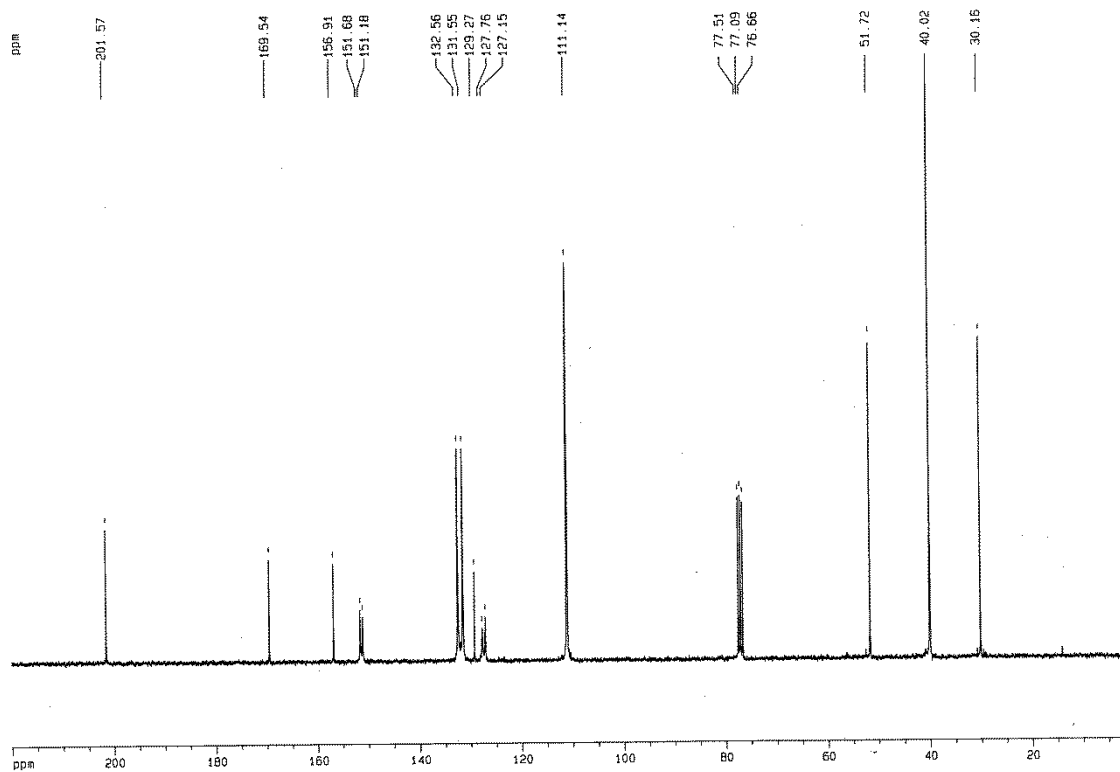
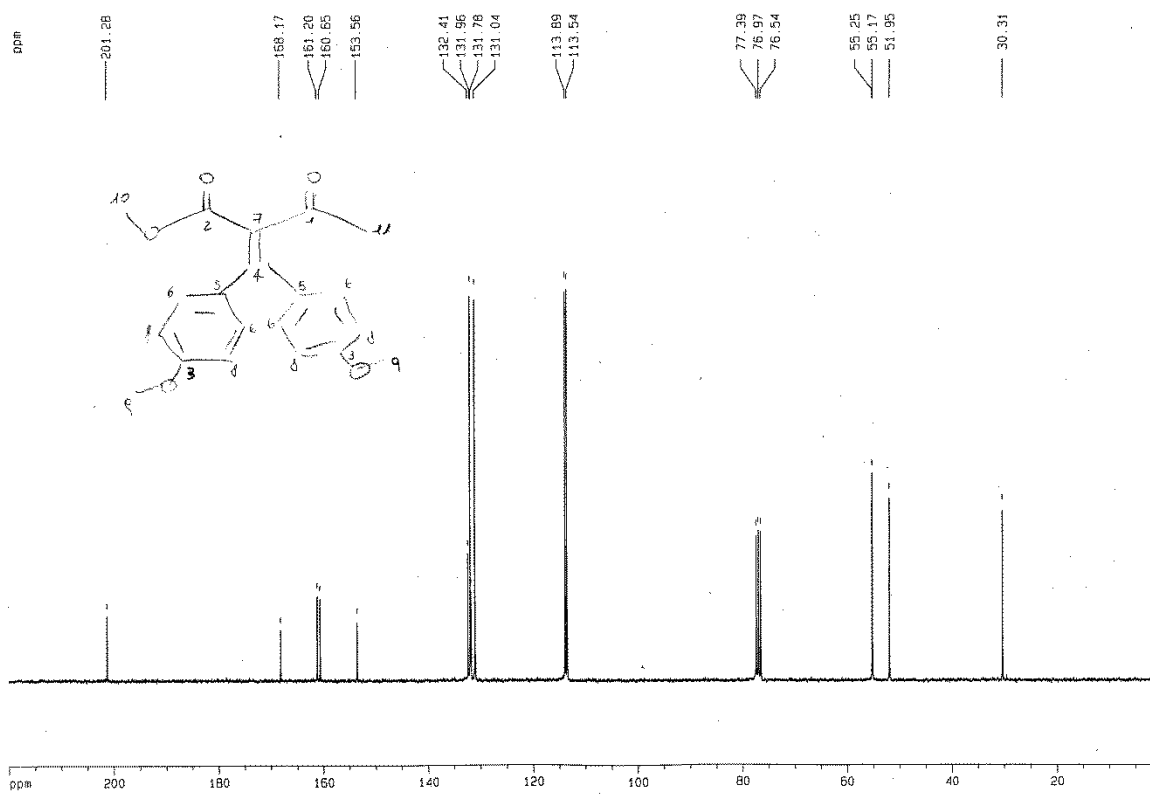^{13}C NMR (CDCl$_3$, 75 MHz)

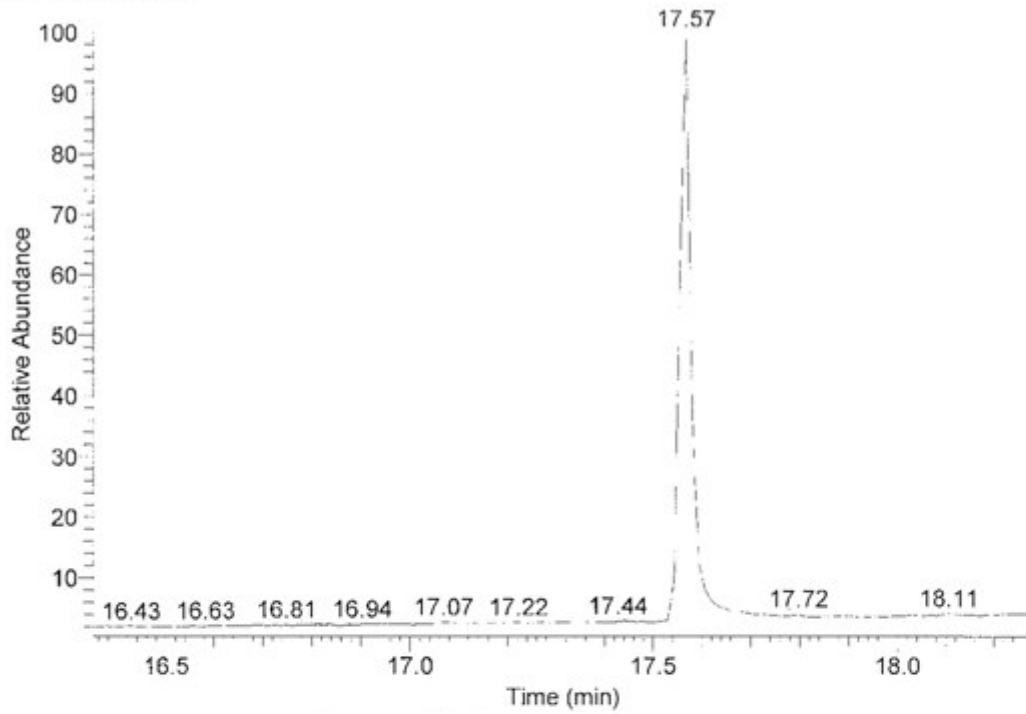^{13}C NMR DEPT (CDCl$_3$, 75 MHz)
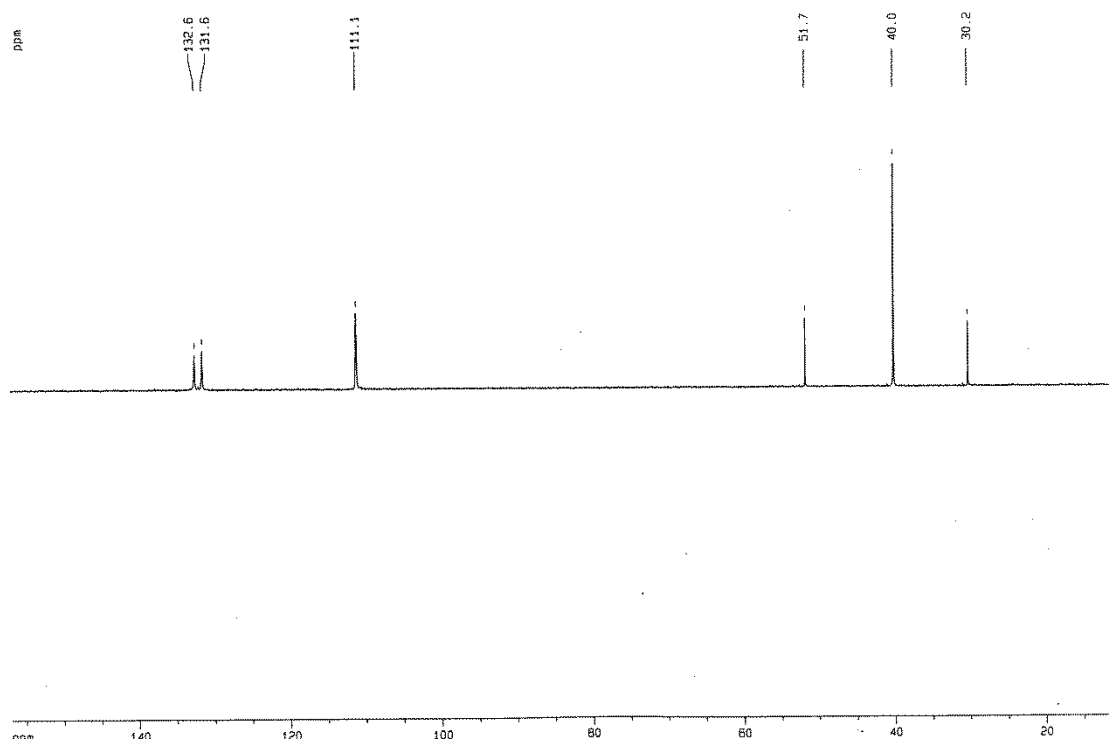
ESI-Mass spectrum
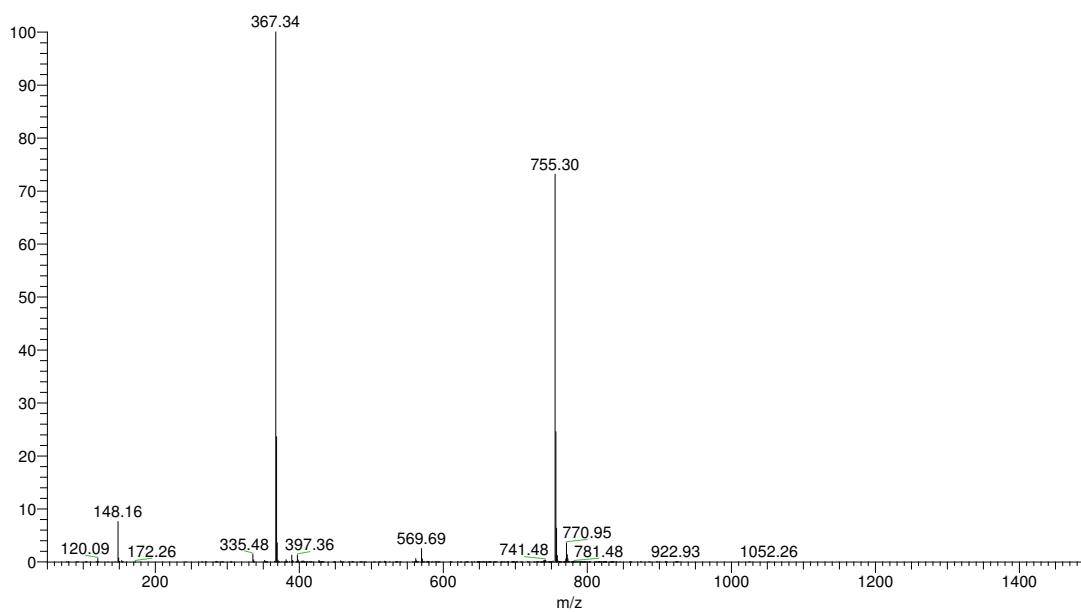
Compound **4e**.
¹H NMR (CDCl₃, 200 MHz)
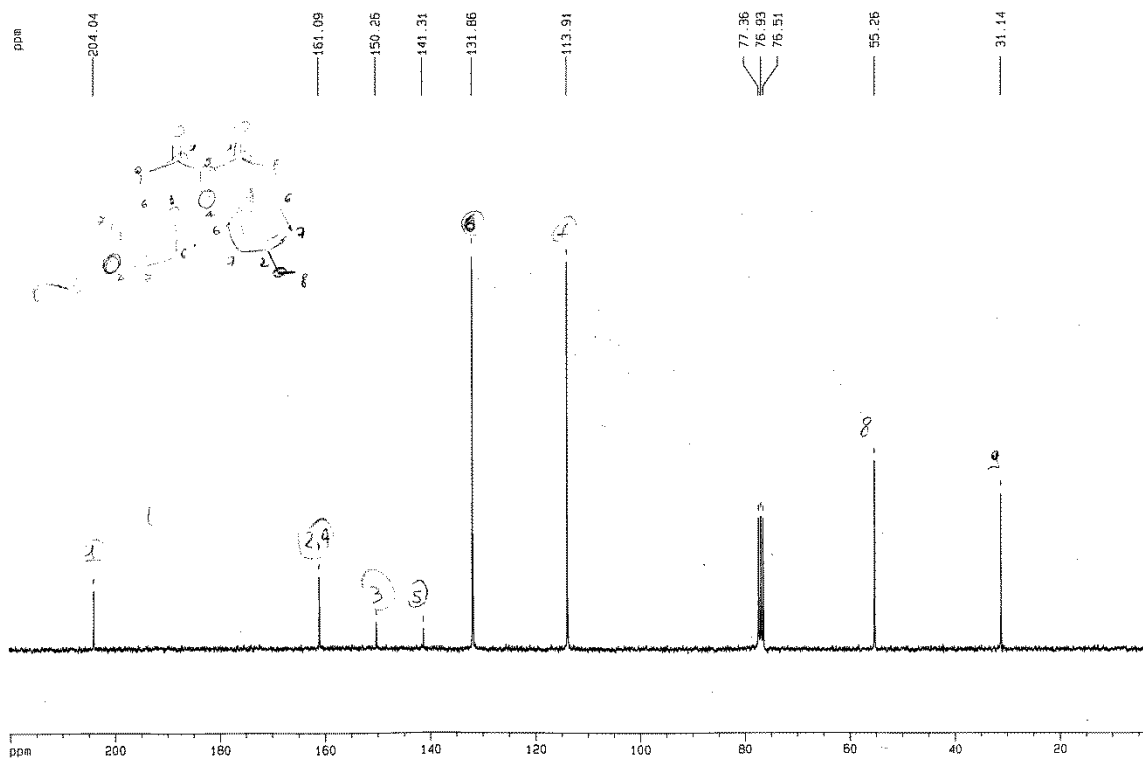
¹³C NMR (CDCl₃, 75 MHz)

Compound **4f**.
^{1}H NMR (CDCl$_3$, 200 MHz)
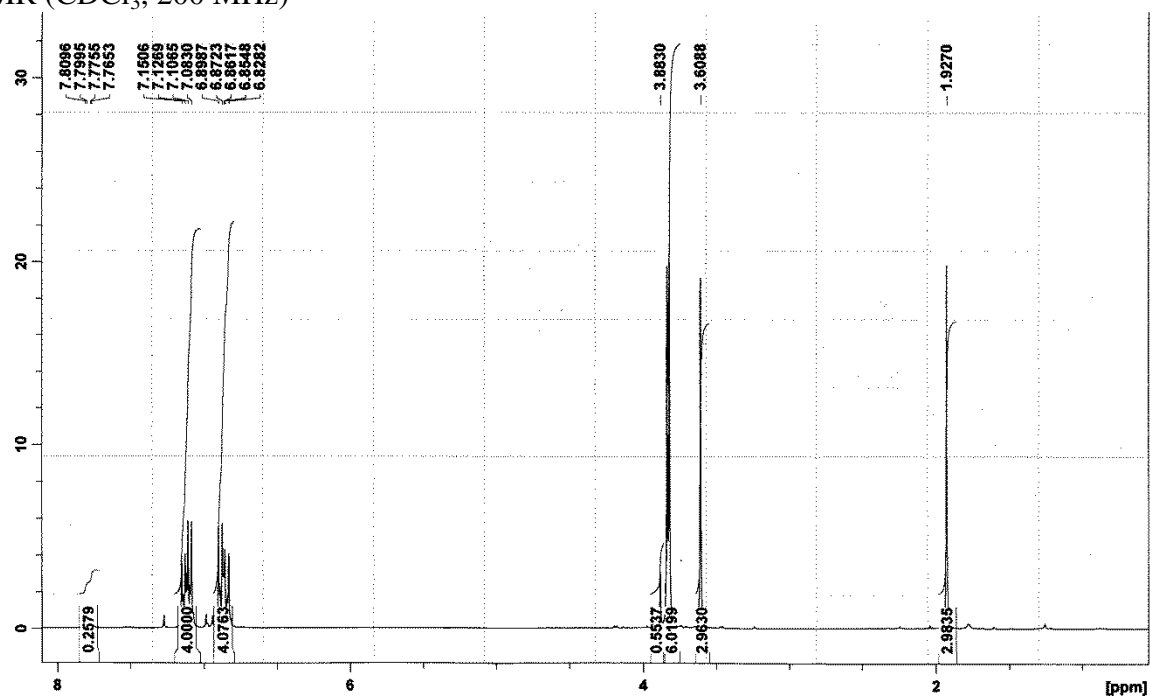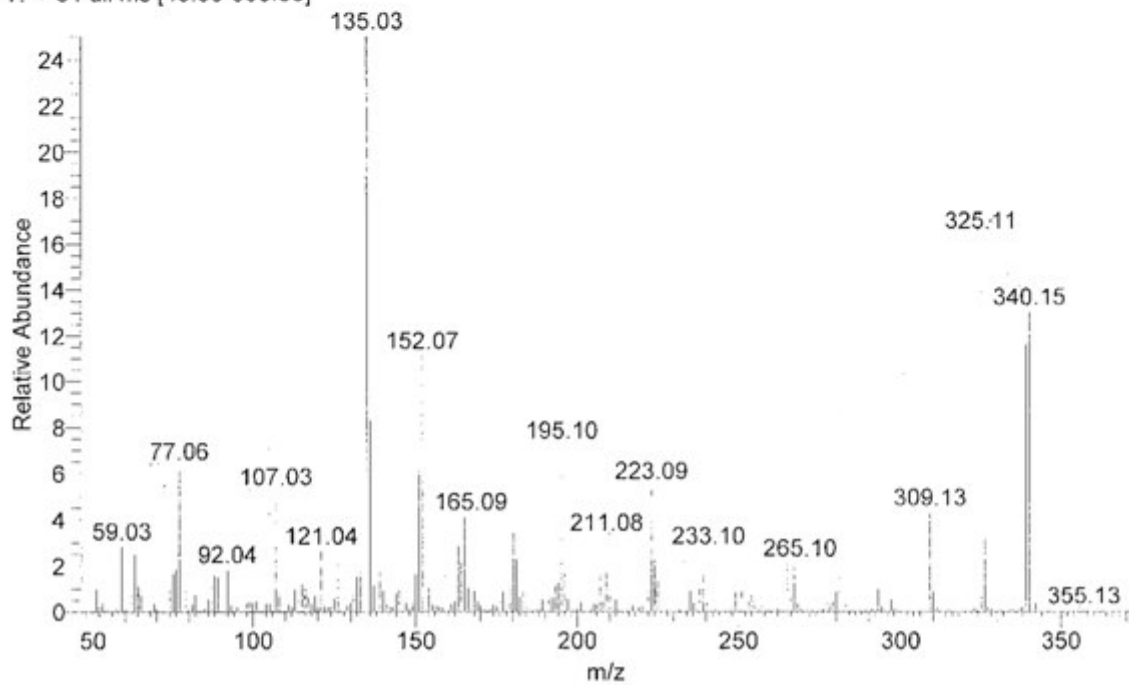

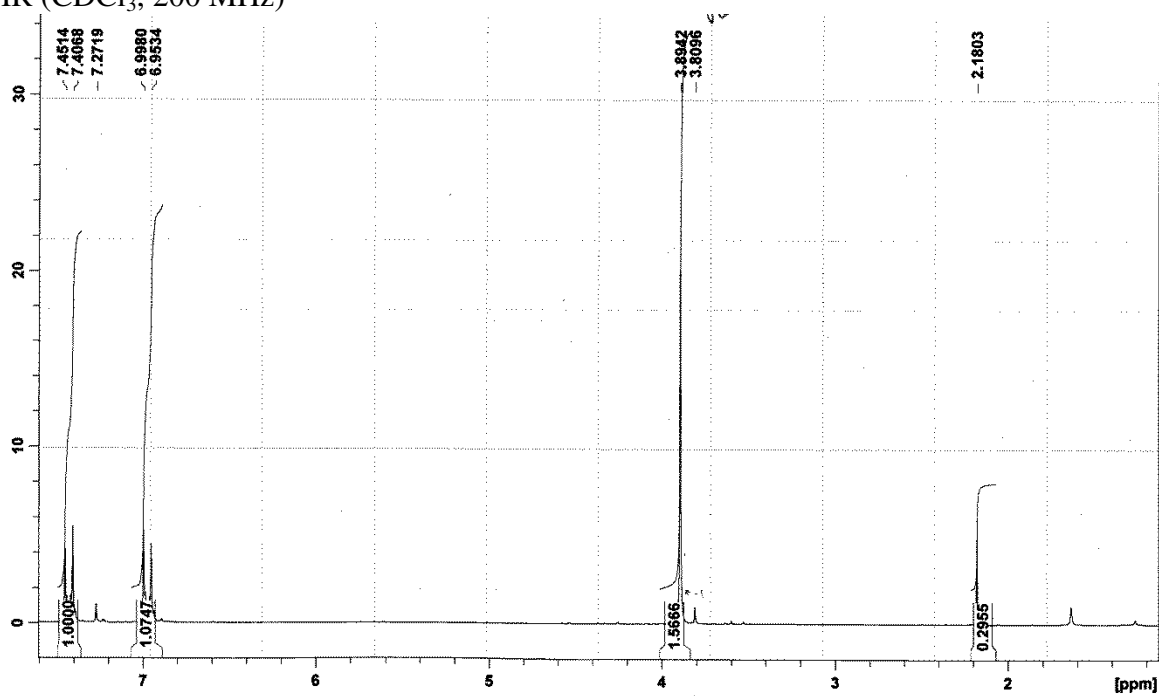
^{13}C NMR (CDCl$_3$, 75 MHz)
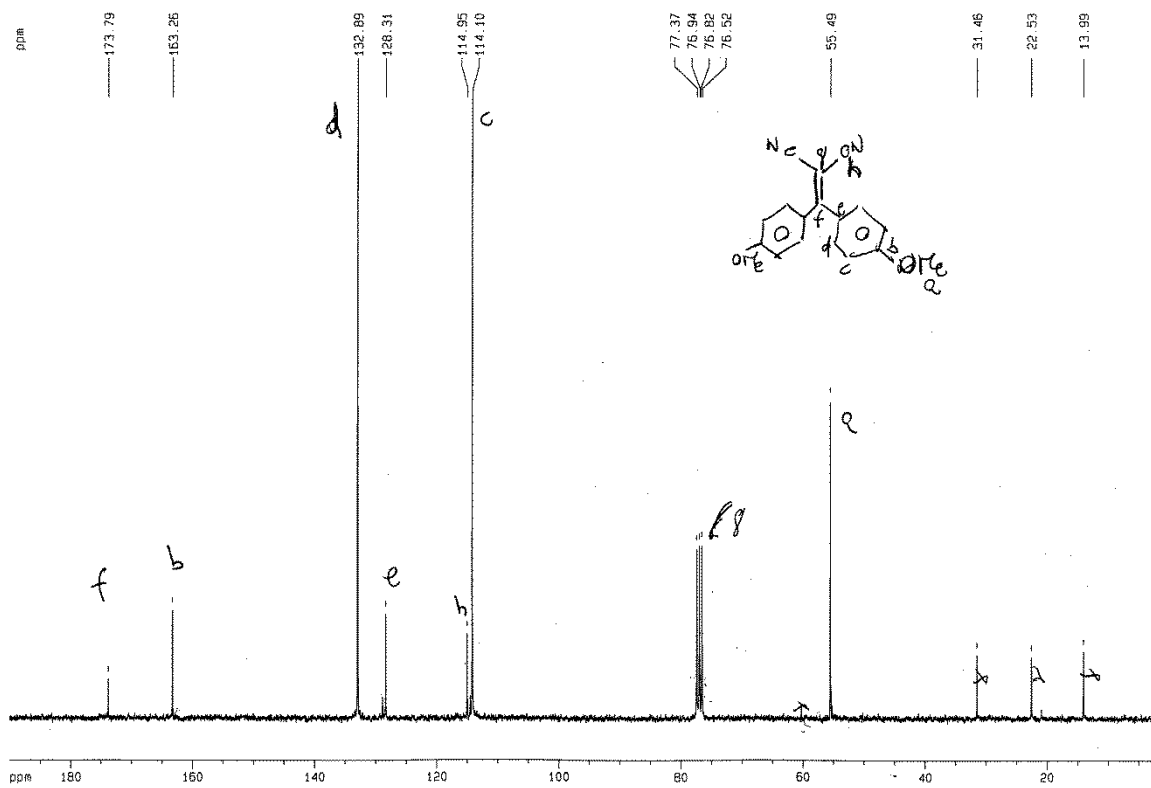
GC- MS

RT: 16.35 - 18.28

17.57

16.43 16.63 16.81 16.94 17.07 17.22 17.44 17.72 18.11

Time (min)

RT: 17.57   AV: 1   NL: 1.50E7
T: + c Full ms [40.00-600.00]

135.03

325.11

340.15

152.07

195.10

77.06

107.03

223.09

165.09

59.03

121.04

211.08

233.10

265.10

309.13

92.04

355.13

m/z

Compound **5b**.

¹H NMR (CDCl₃, 200 MHz)

¹³C NMR (CDCl₃, 75 MHz)

¹³C NMR DEPT (CDCl₃, 75 MHz)